Adenomas and Carcinomas of the Canine and Feline Thyroid

I. Leav, DVM, A. L. Schiller, MD, A. Rijnberk, DVM, M. A. Legg, MD, and P. J. der Kinderen, MD

NEOPLASMS OF THE HUMAN THYROID are a well-studied clinical and pathologic entity. Numerous publications have dealt with their histologic classification and biology. Comparable data concerning thyroid neoplasms in dogs and cats has not been well established, although these tumors have been described in several textbooks and monographs.[1-9]

The purposes of the present study are to: a) classify adenomas and carcinomas of the canine and feline thyroid using specimens from a collection of well-documented cases; b) illustrate gross, microscopic, and ultrastructural features of these tumors; c) review and discuss recent data concerning hyperthyroidism in dogs with carcinoma of the thyroid; d) report for the first time on clinical and morphologic findings in proven cases of medullary carcinoma of the canine thyroid; e) correlate histologic, ultrastructural, and clinical data so that structural functional relationships may be more clearly understood; and f) discuss and compare these findings with features of human thyroid neoplasms. It is hoped that this work will provide oncologists with current information concerning the appearance and biology of thyroid tumors in two domestic animals which share man's environment.

Materials and Methods

Case Material

With the exception of data on hyperthyroidism in dogs and ultrastructural studies of a medullary carcinoma done at the Veterinary College, Utrecht, The Netherlands, all work

From the Departments of Pathology, Angell Memorial Animal Hospital, Tufts University School of Medicine, Massachusetts General Hospital, Harvard Medical School, and New England Deaconess Hospital, Boston, Massachusetts, and Department of Clinical Endocrinology, University Hospital, and The Small Animal Clinic, Utrecht, The Netherlands.

The following also contributed to the research reported in this paper: B. E. Belshaw, DVM, Department of Medicine, Cornell University Medical College, New York, N.Y.; H. J. Wolfe, MD, and R. A. DeLellis, MD, Department of Pathology, Tufts University School of Medicine, Boston, Mass.; E. F. Voelkel and K. M. Gautvik, MD, Laboratory of Pharmacology, Harvard School of Dental Medicine, Boston, Mass.; J. E. Van Dijk, DVM, Department of Veterinary Pathology, State University, Utrecht, The Netherlands; and A. L. Vickery, Jr., MD, Department of Pathology, Massachusetts General Hospital, Boston, Mass.

Supported by Contracts NIH-NCI-E-71-2128 and NO1-CP-33297 from the National Cancer Institute, National Institutes of Health.

Accepted for publication September 21, 1975.

Address reprint requests to Dr. Irwin Leav, Department of Pathology, Tufts University School of Medicine, 136 Harrison Avenue, Boston, MA 02111.

was based on material obtained from the clinical and pathology files of Angell Memorial Animal Hospital, Boston, Mass., from 1949 to 1973. Data from hospital admissions, compiled during a typical sample period of 12 months (July 1, 1962 to June 30, 1963), were used to compare age, breed, and sex distribution with similar information for animals with tumors. A Z-test was used to test for significance of proportion. During the sample period, 7830 dogs and 3562 cats were admitted to the hospital.

For tumor classification, we mainly used the criteria of Meissner and Warren,[10] although other sources were consulted.[9,11-13] Neoplasms were classified according to their predominant histologic pattern. In cases where metastasis was absent, neoplasms were designated as carcinomas when microscopic evidence of vascular and/or capsular invasion was found. A total of 141 neoplasms (44 adenomas and 97 carcinomas) of the canine thyroid were studied; 38 adenomas and 57 carcinomas were from autopsy specimens, while the remainder were surgical biopsy specimens. In addition, 3 carcinomas were diagnosed as neoplasms metastatic from other sites and were designated secondary carcinomas. Both thyroid lobes were available for histologic examination from all autopsied dogs with adenomas and from 44 animals with carcinomas. Ten ectopic thyroid tumors were included in the study and are separately described. Histologic features of five nonchromaffin paragangliomas were compared with the ectopic neoplasms. Fifty-two tumors of the feline thyroid were studied (47 benign lesions and five carcinomas); in all feline cases, specimens were obtained at autopsy and both thyroid lobes were examined microscopically. The majority of animals were killed by an overdose of pentobarbital sodium when the neoplasm was detected, but some died from causes attributable to widespread tumor involvement. In most cases a complete autopsy was done.

Functional Studies

Studies of the functional activity of canine thyroid neoplasms were done at the Veterinary College at Utrecht. For details concerning methodology, the reader is referred to a previous publication.[7]

Scintiscans were done on three animal patients from Angell Memorial Animal Hospital at the Department of Nuclear Medicine, Beth Israel Hospital, Boston, Massachusetts. Prior to scintiscan the animals were given 0.25 to 0.50 mg/lb of promazine hydrochloride (Wyeth Laboratories). Two dogs were given an intravenous dose of 100 μCi freshly prepared carrier-free $Na^{131}I$ in sterile saline. The third dog received 568 μCi intravenously so that autoradiographic studies could be performed on the neoplasm after surgical removal. Autoradiography was done using a previously described technique.[14] All dogs were scanned using an Ohio Nuclear Dual Probe Scanner, and radioactive uptake measurements (RIU) were usually calculated at 4, 24, and 72 hours.

The materials and methods used to induce and study iodine deficiency in beagle dogs have been previously reported.[15,16]

Microscopy

All tissues were routinely processed, cut at 4 to 6 μ, and stained with hematoxylin and eosin. Selected specimens were also stained by the periodic acid–Schiff (PAS) reaction and/or by the alizarin red method for calcium.[17] In addition, a number of tumors were stained with Congo red for the detection of amyloid and by silver nitrate for argyrophilia.[18] At least six replicate sections were studied from a single tumor and in some instances multiple blocks of an individual neoplasm were similarly examined.

The ultrastructure of three carcinomas of the canine thyroid was studied. Tissues were obtained at surgery and immediately diced and fixed in cold 3% glutaraldehyde in 0.67 M cacodylate buffer, pH 7.3, for 2 hours. Specimens were rinsed three times in cold cacodylate buffer, postfixed in 2% osmium tetroxide for 1 hour, dehydrated, and embedded in Epon 812. Thin sections were cut on an LKB ultramicrotome III, double-

stained with lead citrate and uranyl acetate, and examined with a Zeiss EM 952 electron microscope.

One of two specimens of medullary carcinoma of the canine thyroid (Case A—see Clinical Findings and Classification and Description of Canine Thyroid Tumors) was obtained from the Veterinary College at Utrecht. Immediately following surgical removal, the specimen was placed in 4% formol saline at 30 C. Small pieces were stored in this solution at 18 C for 8 months. The tissue was subsequently briefly fixed in 5% glutaraldehyde, postfixed in 2% osmium tetroxide, impregnated with uranyl acetate, and embedded in araldite. Ultrathin sections were cut, mounted on uncoated copper grids, and stained briefly with lead citrate. Sections were examined with a Philips EM 100 C electron microscope.

Immunocytologic Demonstration of Calcitonin-Containing Cells

Before using immunocytologic techniques, we attempted to demonstrate that guinea pig and or rabbit antisera directed against synthetic human calcitonin (reagents used for the immunocytologic method [19]) cross reacted with hypocalcemia-inducing extracts of canine and feline thyroid tissues. Thyroid glands from 5 normal dogs and 3 cats were obtained immediately following death from an overdose of pentobarbital sodium and were quick-frozen on blocks of dry ice. The glands were weighed and immediately homogenized in 0.10 N HCl (20 vol/g). The homogenate was centrifuged at 10,000*g* for 30 minutes, and aliquots of the supernatant were taken. Aliquots were diluted to 0.5 cu cm in 0.01 N HCl and 1% bovine serum albumin and assayed for hypocalcemic activity according to the method described by Cooper *et al.*[20] Remaining aliquots were diluted in 0.10 M Tris-HCl at pH 7.5 and a radioimmunoassay (RIA) utilizing a guinea pig anti-human calcitonin reagent was used to detect the hormone.[21]

Sections from thyroids from 4 normal dogs and 3 normal cats were obtained immediately following death from an overdose of pentobarbital sodium and fixed in 10% buffered formalin. They were routinely processed, embedded in paraffin, cut at 4 to 6 μ, and stained by the immunoperoxidase bridge technique for the identification of calcitonin-containing cells.[19] Control reactions were the replacement of the primary antisera with normal rabbit or guinea pig sera and the absorption of the primary antisera with synthetic human calcitonin at the zone of antigen–antibody equivalence. Both procedures resulted in the loss of positive staining in previously reactive cells. This method was subsequently applied to fifteen canine and one feline thyroid neoplasms.

Results

Analysis of Cases

The average age for dogs with adenomas of the thyroid was 10.7 years, with a range of 7 to 15 years, while for animals with carcinomas it was 9.0 years, with a range of 4 to 18 years. The ages of 40% of dogs admitted to Angell Memorial Animal Hospital during 1962 to 1963 fell within these ranges. Primary adenomas were found in 25 males (57%) and 19 females (43%); 1 male and 9 females were neutered. Forty-three males (46%) and 51 females (54%) had primary carcinomas; 4 males and 41 females were neutered. No significant differences were found between these values and the sex distribution of the sample period. In agreement with past studies,[4,7] tumors of the thyroid occurred more frequently in boxers than in any other type of dog (41% of adenomas, 20% of carcinomas). These figures differed significantly from the percentage of boxers (4.9%

of all breeds) admitted to the hospital during the period sampled ($P < .0001$).

The average age for cats with benign tumors was 12.4 years, with a range of 4 to 22 years; that for 5 cats with malignant thyroid neoplasms was 15.8 years with a range of 13 to 18 years. Although the ages of 27% of cats admitted to the hospital during the sample years fell within the range for adenomas, only 4.5% were in the older age groups observed for cats with carcinomas. Twenty-six (55%) cats with benign tumors were males (16 neutered) and 21 (45%) were females (19 neutered); these values closely approximated the sex distribution of cats admitted to the hospital during the sample period. All cats with carcinomas were male (4 neutered, 1 intact). Three of 52 cats with thyroid tumors were purebred.

Clinical Findings—Canine Cases

Benign neoplasms of the canine thyroid are small, focal lesions, not commonly detected during life. In 7 cases, however, these tumors were cystic and large enough to be noted in the living animal. Retrospectively, no conclusive evidence of hypo- or hyperthyroidism was found in the clinical records of any dogs with adenomas.

The majority of dogs with thyroid carcinoma (61%) were brought to the hospital because of a mass in the cervical region. In those cases where the primary neoplasm became large enough to be noticed, metastases were frequently present. Respiratory distress was the most common presenting clinical sign (42%) in dogs with carcinoma. In the majority of instances this sign could be correlated with metastases in the lung or compression of the trachea by the neoplasm.

Protein-bound iodine (PBI) and total iodine (TI) levels were determined in 18 cases; values for 13 animals were within normal ranges. (Normal PBI values for dogs at Angell Memorial Animal Hospital: average, 2.9 μg%; range, 1.1 to 4.0 μg%. Measurements of TI were always done along with PBI to exclude the possibility of exogenous contamination.) In the remaining 5 cases the level of PBI (average, 6.0 μg%; range, 4.7 to 7.0 μg%) was elevated. Three of the 5 animals had signs consistent with hyperthyroidism. Scintiscans done on 2 of the 3 dogs were similar to those seen in thyrotoxic animals described by Rijnberk.[7]

Hyperthyroidism in Dogs

In recent years a number of investigators have described cases of thyrotoxicosis in dogs with carcinoma of the gland.[22-26] The best documented study of hyperfunction in dogs with thyroid neoplasms is the work of Rijnberk.[7] The investigator studied various parameters of iodine

metabolism in 58 dogs with thyroid tumors. In 13 animals the neoplasm was associated with a clinically hyperfunctional state which produced measurable alterations in iodine metabolism. In some cases the onset of clinical signs was abrupt, while in others the neoplasms developed insidiously. Polydipsia and polyuria, unassociated with primary kidney disease or any other metabolic disorder, were the most frequent signs exhibited by these animals. The majority of dogs lost weight despite an increased intake of food. Weakness and fatigue were reported in 8 animals. Most animals exhibited an intolerance to slight elevations in ambient temperature and sought cool places. Restlessness, characterized by continuous pacing, was also common. The heart rate was considered high (average 133 beats/min) and in 3 dogs, electrocardiographic recordings showed high voltage in all leads.

Twelve of the 13 animals had unilateral thyroid neoplasms. Although all tumors were, microscopically, carcinomas, they were generally small and had not metastasized or invaded adjacent tissues. One of these 12 animals, with clinical signs of hyperthyroidism, had exacerbation of this condition after ipsilateral recurrence 1 year following a hemithyroidectomy. In the remaining dog, hyperthyroidism was due to an ectopic thyroid carcinoma located on the midline just below the anterior portion of the larynx.

In his studies, Rijnberk utilized scintiscans as one criterion of autonomous hypersecretion by canine thyroid neoplasms (Figures 1 and 2). Although all clinically hyperthyroid dogs had suppressed contralateral lobes caused by the effect of elevated serum hormone on thyrotropin release, some dogs with similar scintiscan findings did not exhibit these signs. In these cases, thyroid hormone secretion by the neoplasm apparently caused decreased uptake in the nonneoplastic lobe, but the hormone was not produced in amounts sufficient to evoke a hyperthyroid state. Further increases in circulating hormone levels would probaably have resulted in the appearance of toxic signs. Following the administration of exogenous thyrotropin the now-stimulated nonneoplastic lobe took up radioiodine (Figure 2).

Scintiscans were divided into three categories according to radioiodine distribution in the neoplasm: a) diffuse ^{131}I accumulation, b) extensive "cold" areas, c) no ^{131}I accumulation. Scintiscans of animals with suppressed contralateral lobes were further divided as clinically hyperthyroid (I) or euthyroid (II), while scans from dogs without suppressed contralateral lobes and those from animals with bilateral tumors were designated as III and IV, respectively.

When compared with 14 normal animals of similar body size, those

with functional neoplasms had elevated thyroidal iodine turnover indexes (turnover index = ratio of 24-hour and 72-hour radioactive iodine uptake values), but an overlap in value ranges was observed. The radioactive iodine uptake (RIU) curve for hyperthyroid dogs peaked sharply when measured under 4 hours and returned to normal ranges in 24 hours (Text-figure 1), thus affording a clear separation between toxic and normal animals. The highest hormonal iodine (HI) and PBI values were found in hyperthyroid dogs (Text-figure 2). In general, euthyroid animals with suppressed contralateral lobes did not have the high PBI and HI values seen in those with toxic signs. Discrepancies between PBI and the combined sum of HI and iodinated amino acids (IAA) were frequent in cases of hyperthyroidism, suggesting the presence of circulating iodoproteins (Text-figure 2). This concept was supported by ultracentrifugation studies of two hyperfunctioning neoplasms, which revealed large amounts of 4S components and minor quantities of 19S protein. In most species, the 19S component is considered to be thyroglobulin,[27] while the more slowly sedimenting molecules found in tumors may be subunits arising from defective synthesis.[28] Following treatment with radioiodine or surgical removal of the neoplasm, thyrotoxic signs disappeared in all animals and parameters of iodine metabolism returned to normal.

Medullary Carcinoma of the Canine Thyroid

Syndromes associated with medullary carcinoma of the human thyroid have been well studied,[29-31] while documented cases of medullary carcinoma of the canine thyroid have not been reported. The following

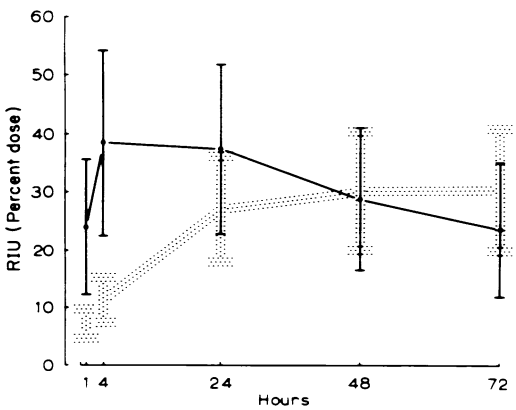

TEXT-FIGURE 1—Mean radioactive iodine uptake curve (± SD) of 13 hyperthyroid dogs (*solid line*) compared with the RIU curve of 14 normal dogs of comparable body size (*dotted lines*).

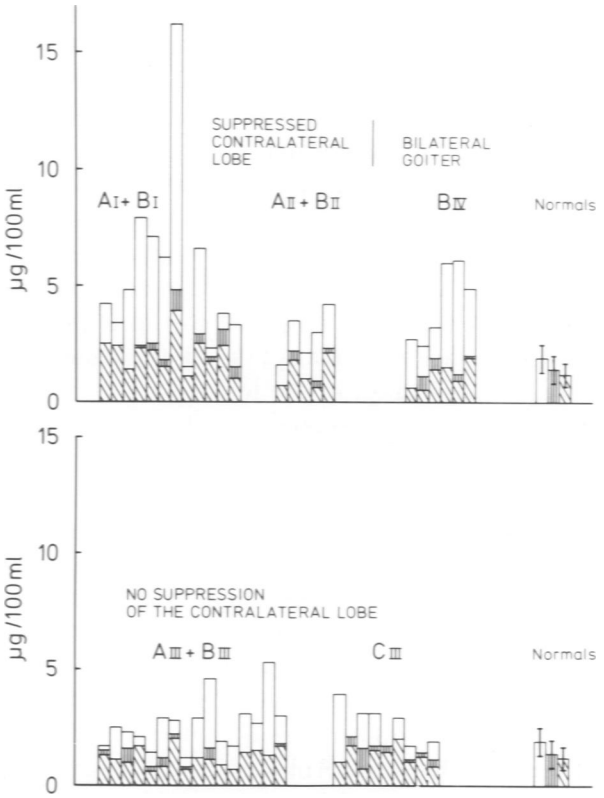

TEXT-FIGURE 2—Circulating protein-bound iodine (PBI), hormonal iodine (HI), and iodinated amino acids (IAA) values in dogs with thyroid carcinoma. Values are grouped according to scintiscan category and clinical status. All clinically hyperthyroid animals had AI and BI scans. (PBI, *open columns*; IAA, *striped columns*; HI, *hatched columns*)

discussion summarizes the clinical findings in 2 cases of canine medullary carcinoma. The morphologic features of both tumors are discussed in Classification and Description of Canine Thyroid Tumors.

Case A. A 7-year-old intact female collie was brought to the clinic because of watery diarrhea that was first noted 3 months prior to presentation. Two months before, a small oval mass had been noticed in the right cervical area and had since doubled in size. There were no signs suggestive of hyperthyroidism.

The serum calcium level (9.8 mg%) was just below the normal range (normal serum calcium range for dogs at the Veterinary College of Utrecht, 10.6 to 12.4 mg%), but the results of other routine laboratory studies were normal. Radioiodine uptake in the neck area was low, occurring only in the caudal pole of the mass and in the contralateral lobe. The uptake curve showed a normal slope, and the $PB^{131}I$ was also normal (0.13% dose/liter).[7] These findings were interpreted as being caused by a poorly differentiated neoplasm displacing unaffected thyroid tissue.

A firm, oval mass was surgically resected from the right cervical area. Diarrhea began gradual clearing on the second postoperative day and has not recurred. To this date, almost 3 years following the removal of the mass, the animal remains in good health. All laboratory values including serum calcium are normal.

Case B. A 12-year-old neutered female spaniel cross was first seen at Angell Memorial Animal Hospital because of severe polydipsia of a month's duration. At this time, clinical tests revealed hyperglycemia and glucosuria, and a diagnosis of diabetes mellitus was made. In addition, a small oval mass was palpated in the region of the right thyroid lobe. A scintiscan showed poor uptake by the mass, with most of the radioactivity being concentrated in the left lobe.

The dog was regulated for diabetes by insulin administration. Three months later a bilateral thyroidectomy was performed. The parathyroids were identified and left in place. Following surgery the animal was given levothyroxine (Norden Laboratories) daily. The dog had an uneventful recovery until 7 months after surgery, when progressive episodes of weakness and ataxia developed. Neurologic findings on admission were limited to periodic disorientation and mild proprioceptive deficit in the right limbs. A seizure occurred shortly thereafter that progressed to a tonic type, lasting about 5 minutes. Clinical tests were normal with the exception of a low serum calcium level (5.0 mg%) (normal ranges for dogs at Angell Memorial Animal Hospital: serum calcium, 8.4 to 11.2 mg%; serum phosphorus, 2.2 to 4.0 mg%) and slightly elevated phosphorus level (5.6 mg%). The animal was treated by the intravenous and oral administration of calcium and vitamin D. All neurologic signs disappeared after 7 days of therapy. This treatment was stopped after 3 months because of hypercalcemia and azotemia. Serum calcium values returned to normal in 9 days. Thoracic radiographs failed to disclose any abnormalities, and to this date the animal is clinically normal. All laboratory values have been normal with the exception of the blood urea nitrogen, which has remained elevated.

Calcitonin Studies

The extracts of normal canine thyroid had a hypocalcemic effect in the bioassay test, and the active substance was detectable by radioimmunassay. The average content of calcitonin of the canine gland was 0.37 MRC milliunits/mg of tissue wet weight (bioassay). (The standard error limits of these estimates were $X/\div$ 1.1 to 1.3. The factors following the symbol $X/\div$, when multiplied by and divided into the potency estimate, give the standard error of the estimate.) These methods

thus established the presence of a substance with hypocalcemic activity in the canine thyroid and gave indirect evidence that guinea pig antisera directed against human calcitonin could be used to assay for the hormone in dogs.

We utilized the immunoperoxidase technique to study the distribution of calcitonin-containing cells (C) cells in the canine thyroids. Unlike human C cells, which are primarily interfollicular and located in the middle third of the lateral thyroid lobes,[33] those of the dogs were mostly in a parafollicular position and evenly dispersed throughout the gland (Plate 1).

The RIA and bioassay techniques failed to detect calcitonin in feline thyroids. However, the immunocytologic methods demonstrated weakly positive cells in these tissues. Feline C cells appeared to be fewer in number than those in canine thyroids, were dispersed throughout the gland, and located primarily between follicles (Figure 3). We conclude that feline calcitonin is probably weakly cross reactive with guinea pig antisera, and that the hormone content of the feline gland is below the resolution of the bioassay.

Histologic Response of the Canine Thyroid to Iodine Deficiency

In some instances of adenomatous human goiter the histologic appearance of the gland may closely resemble that of a carcinoma.[10] Similar alterations have been reported to occur spontaneously in the glands of dogs living in areas of the world where iodine is deficient[34] Belshaw[15,16] has recently studied the histologic responses and radioiodine metabolism of canine thyroids from beagle dogs fed diets deficient in iodine. The morphology of thyroids from 3 animals, each from a different experimental group, are illustrated in Figures 4 and 5. A spectrum of changes ranging from mild proliferation to severe hyperplasia was seen. The mildest alterations were papillary infoldings of follicular epithelium (Figure 4). At this point, scalloping of colloid was readily visualized within follicles. As the hyperplastic process became more pronounced, follicular lumens were filled with cells. In intensely hyperplastic glands, follicular cells were practically devoid of PAS-positive droplets and assumed an almost entirely compact cellular pattern, reminiscent of the histologic appearance of some adenomas and carcinomas of the canine thyroid (see Classification and Description of Canine Thyroid Tumors) (Figure 5). Thus, severe hyperplasia may be histologically identical to adenomas and closely resemble carcinomas of the canine thyroid. The absence of vascular and capsular invasion should establish the benign nature of the lesion.

Classification and Description of Canine Thyroid Tumors

General Findings. In the absence of metastases, thyroid tumors were designated as adenomas when they lacked the critical features of capsular and vascular invasion. In a few cases, multiple nodules occurred within a single lobe, making it difficult to distinguish between hyperplasia and true adenomas. Foci that were at least partially circumscribed by a capsule, compressed the adjacent tissue, and differed histologically from the remaining thyroid were classified as adenomas, while those which lacked these features were considered to be hyperplastic lesions.

Bilateral involvement was present in only 5 animals, and no predilection for either lobe was noted in the remaining cases. With the exception of one tumor, adenomas were classified as follicular neoplasms. Patterns comparable to those observed in humans were seen.

Twenty-eight of 44 autopsied dogs (64%) had a unilateral carcinoma, while bilateral involvement was found in 16 cases (36%). When carcinoma was bilateral the neoplastic process was extensive. It was therefore not possible to determine whether tumors had arisen in both glands or metastasis occurred from one lobe to the other. When carcinoma was unilateral, no predilection for either lobe was noted.

The size of a carcinoma, measured at autopsy, appeared related to the presence of metastases. A difference in the percentage of animals with metastases was evident when tumors less than 21 cu cm were compared with those exceeding this size (Table 1). It therefore appears that tumor size is a critical factor in the establishment of distant metastases. However, even in the absence of metastases, neoplastic emboli may enter the circulation while tumors are quite small. In the present series, 4 autopsied dogs had small, unilateral, seemingly well-encapsulated neoplasms that were classified as carcinomas. Metastases were not found in any of the animals. On cut surface, these tumors were sharply demarcated from the surrounding tissue and grossly resembled solid adenomas. Histologically, two of the neoplasms had a microfollicular pattern. Along the subcapsular zone cells were less uniform and assumed a compact cellular arrangement. Cells comprising the other two neoplasms were

Table 1—Measurements of Thyroid Carcinomas in Relationship to Metastasis

Tumor volume (cu cm)	No. animals autopsied*	Percent with metastasis
1-20	14	14
21-100	19	74
101-500	9	100
501-1000	4	100
1001-1500	3	100

* Measurements were not recorded in 8 cases.

Table 2—Frequency of Organ Involvement*

Anatomic site	Percentage of animals
Lung	77
Regional lymph node	51
Local invasion†	49
Adrenal	14
Kidney	14
Heart muscle	9
Liver	6
Intestine	6
Skin	6
Brain	3
Spleen	3
Mesentery	3
Diaphragm	3

* Data is based on 35 autopsied dogs with metastatic carcinoma of the thyroid.
† Includes invasion of thyroidal, jugular and maxillary veins, esophagus, trachea, larynx, omohyoid muscle, and vertebra.

pleomorphic and arranged in cords or irregular follicles. All four tumors appeared encapsulated, but serial sections revealed evidence of capsular and vascular invasion (Figures 6 and 7). Hazard and Kenyon [35] described tumors of the human thyroid which are grossly and microscopically similar to these canine neoplasms. They designated these *encapsulated angioinvasive carcinomas.*

Metastasis occurred in 35 of 57 autopsied dogs, the lung and regional lymph nodes being most often affected (Table 2). All but 8 animals with metastasis to other sites also had tumor in the lungs. In the remaining cases, carcinoma had spread to adjacent structures or regional lymph nodes. Neoplastic emboli were frequently found in the internal jugular and thyroidal veins. Past reports have documented the frequency of pulmonary metastasis and emphasized the hematogenous route as the main means by which carcinoma of the thyroid is disseminated in dogs.[36-38] Local extension to adjacent organs such as the trachea and esophagus was common (Figure 8). In 1 animal the tumor invaded the cervical vertebrae, but distant metastasis to bone was not observed in this or any other cases. Thus, contrary to the situation in humans, where metastasis of thyroid carcinoma to bone is not uncommon, it appears to be rare in dogs.[38]

Unlike carcinomas of the human thyroid, a papillary pattern was rare in canine neoplasms. Most canine carcinomas had a mixed appearance in which cells were arranged in both follicular and compact cellular patterns. The degree to which either pattern was represented often varied considerably within a single tumor. Furthermore, the dominant histologic pattern seen in the primary neoplasm was not always observed in the

metastases. Thus, a malignancy with mainly a follicular pattern might yield metastatic foci with a compact cellular appearance and vice versa.

Due to the difficulty in obtaining accurate follow up information, retrospective data could not be gathered concerning the influence of histologic type on the survival of dogs with carcinoma of the thyroid. In the few cases where such information was available, it was our impression that a follicular pattern was usually associated with a more rapid, less favorable course than was the case for neoplasms in which a compact pattern predominanted.

Nuclear pleomorphism and abundant mitoses were uncommon in the majority of differentiated canine carcinomas, but exceptions did occur. Nuclei exceeding 5 to 8 μ in diameter (the usual size range for most neoplastic thyroid cells) were occasionally found.

A single, homogeneous, eosinophilic inclusion was noted in a number of large nuclei (see Figure 24). Similar intranuclear inclusions, considered to be cytoplasmic invaginations, have been observed in papillary thyroid carcinomas of humans.[39] Fibroplasia in response to invading cells was a variable finding in canine thyroid carcinomas. The intensity of this reaction ranged from a relatively mild production of collagen to a severe fibrosis. Large areas of hemorrhagic necrosis were common in follicular neoplasms, as were spicules of woven and lamellar bone.

Adenoma of the Canine Thyroid. FOLLICULAR ADENOMA. Adenomas of the canine thyroid appear as either solid (Figure 9) or cystic (Figure 10) masses. Solid adenomas were round or ovoid and were a few millimeters to several centimeters in diameter. Although a well-delineated capsule was seldom noted, they were frequently solitary and distinct from the compressed adjacent thyroid. They were usually soft and ranged from cream to red-brown. The large cystic adenomas were turgid and had smooth exterior surfaces covered by an extensive network of blood vessels. When cut they exuded a clear amber or blood-tinged fluid. The cut surface was characterized by a central cavity with a smooth or rugose lining, often containing flecks of gritty, hard white tissue (Figure 10).

Microscopically, adenomas were characterized by either small (microfollicular) or large (macrofollicular) irregular follicles containing varying amounts of colloid (Figures 11 and 12). The majority of tumors had a microfollicular pattern consisting of uniform cells that formed

Table 3—Adenomas of the Canine Thyroid

Pattern	No. of neoplasms
Follicular	43
Papillary	1

follicles which varied in size, shape, and content (Figure 11). Foci of compactly arranged cells were frequent and some resembled oxyphils commonly seen in human adenomas. However, cytoplasm of canine cells was lightly acidophilic and lacked the pronounced granularity characteristic of human oxyphils. One small neoplasm was almost entirely composed of these cells arranged in a compact cellular pattern. Cells of macrofollicular tumors tended to be larger (10 μ) and have less uniform nuclei than those of microfollicular tumors. Mitoses were not seen in any adenomas.

Thirteen follicular tumors each contained a large, central cyst filled with mineralized necrotic debris and red blood cells. Cysts were lined by a dense fibrous capsule from which projected fronds of uniform cells arranged in follicular and/or compact cellular patterns (Figure 13). Since cysts were seen in many small solid adenomas, it is likely that cycles of continued growth accompanied by degenerative changes were responsible for the eventual appearance of the tumors.

Papillary Adenoma. This neoplasm occurred as a soft, unilateral, solitary focus, characterized microscopically by branching thin, vascular connective tissue septa lined by uniform cuboidal cells similar to those of microfollicular adenomas (Figure 14). The surrounding spaces contained colloid, cellular debris, and red blood cells. A thin capsule partially surrounded the tumor, demarcating it from the compressed adjacent tissue. Foci of calcium deposits were common and found either joined to cell clusters or free within spaces. The opposite thyroid lobe was normal.

Carcinomas of the Canine Thyroid. Follicular Carcinoma. Follicular carcinomas were characterized by a firm, nodular external surface with focal softer areas. The cut surface frequently contained an irregular central region filled with soft, dark red caseous material, surrounded

Table 4—Carcinomas of the Canine Thyroid

Pattern	No. of neoplasms
Follicular	16
Compact cellular*	15
Mixed follicular–compact cellular	56
Mixed papillary–follicular	1
Medullary	2
Anaplastic†	
Spindle cell	1
Giant cell	2
Diffuse small cell	1
Secondary carcinoma	3

* Synonymous terms: solid carcinoma,[9] predominantly solid carcinoma.[4]

† These neoplasms were classified according to the histologic criteria of Meissner and Warren.[10]

by firm, cream-colored tissue (Figure 15). Hard, gritty spicules were common in and around the soft central regions. Metastatic foci were cream colored and usually firm, but sometimes had depressed soft centers.

Microscopically, the majority of neoplastic cells formed follicles, although a minor compact arrangement was also usually present. Some neoplasms had a predominantly microfollicular pattern, while others were characterized by larger, irregularly shaped follicles (Figures 16 and 17). Foamy, vacuolated colloid was frequently found in the lumens of larger neoplastic follicles but was absent in microfollicles (Figures 16 and 17). In general, two types of cells comprised follicular carcinomas. The larger type (15 to 20 μ) usually formed the more distinct follicles while smaller cells (10 μ) were frequently arranged as microfollicles. The larger cells were characterized by round, vesicular nuclei with prominent nucleoli (Figure 17). The cytoplasm was eosinophilic, finely granular, and comprised about half of the total cell volume. Bright, PAS-positive secretory droplets were numerous. The smaller cells had vesicular or hyperchromatic oval nuclei and a scant amount of cytoplasm that usually lacked PAS-positive droplets.

The fine structure of neoplastic follicles was studied and cell types are illustrated (Figures 18 and 19). One specimen was derived from a dog with hyperthyroidism with a suppressed contralateral lobe. Autoradiographs of this neoplasm revealed radioiodine concentration in the follicular portions of the tumor and, to a lesser extent, in compact cellular regions (Figure 18). On ultrastructural examination, cells were columnar and had numerous microvilli projecting from their apical surfaces (Figures 18 and 19). The basement membrane appeared flat. Cell junctions were most often tight, but sometimes a thin intercellular space was noted. Nuclei were round to ovoid, but occasionally had a folded appearance. Chromatin was usually clumped along the nuclear membrane and nucleoli were often distinct. Due to dense accumulations of free ribosomes, some cells appeared to have a more darkly stained cytoplasm than others. Mitochondria varied in shape and were dispersed throughout the cells. Dense bodies were common and differed in size and shape. Colloid droplets were found along the apices of most cells (Figure 19). The rough endoplasmic reticulum (RER) was dilated and filled with a light staining granular material (Figure 19). Golgi complexes were dispersed in small, dense cisternal aggregates that were somewhat obscured by other organelles. Microvesicles were numerous.

Figure 20 illustrates regions from another carcinoma with a microfollicular pattern. Nuclei were round with finely dispersed

chromatin and distinct nucleoli. Cytoplasm was scant but densely packed with free ribosomes, profiles of RER, numerous mitochondria, and sometimes a well-developed Golgi complex. Unlike the previous tumor, colloid droplets were absent, but a few large, irregular, dense bodies were present in many of the cells. Intercellular spaces were often prominent and enclosed villous cytoplasmic projections from the apices of adjacent cells (Figure 20). This arrangement simulated the appearance of microfollicles as seen by light microscopy.

1. Compact cellular carcinoma. These neoplasms were firm and usually had a smooth external surface. When cut they were uniformly cream colored, finely lobulated, and lacked the large, hemorrhagic foci seen in follicular carcinomas (Figure 21). Metastases resembled those of follicular carcinomas.

Microscopically, these tumors were composed of densely packed sheets of randomly arranged cells divided into lobules by thin strands of fibrous connective tissue and small blood vessels (Figure 22). A minor follicular component was sometimes noted. Generally, the cells were about 12 μ, round or polygonal, and sometimes appeared strikingly uniform within a single neoplasm (Figure 22). Nuclei tended to be vesicular and located centrally. The cytoplasm was lightly eosinophilic, and granular or foamy. Nuclear pleomorphism and large nucleoli were seen, but these findings were uncommon. Mitoses were rare. Clusters of Hurthle cells were found in a few compact cellular carcinomas (Figure 22). Cytoplasmic PAS-positive secretory droplets were rarely observed. Eight compact cellular neoplasms were negative when tested for argyrophilia, amyloid, and the presence of immunoreactive calcitonin.

The fine structure of a compact cellular carcinoma is illustrated in Figure 23. Both light and dark staining cells were distinguished, but the only apparent difference between them was the number of free ribosomes. Nuclei occupied the major portion of the cells and often contained large nucleoli. The amount of clumped chromatin along nuclear margins varied among cells. Nuclear outlines were fairly smooth and round to ovoid. There was little intercellular space; when present it sometimes contained basement membrane–like material. RER was abundant and usually associated with numerous mitochrondria. Multilaminated bodies were found in some cells and were considered to be abnormal mitochondria. Golgi complexes were dispersed and seen as small flat cisternae. Microvesicles and dense bodies were occasionally found. Although infrequent, long dense intracytoplasmic tubules were seen (Figure 23).

2. Mixed follicular–compact cellular carcinoma. These neoplasms were firm and had external and cut surfaces similar to those found in pure

follicular neoplasms. Flecks of dense, gritty tissue were common. Metastases resembled those seen in follicular and compact cellular neoplasms.

Tumors were classified in this manner when both patterns were approximately equally represented (Figure 24). It was necessary to examine several sections of an individual neoplasm before this estimation could be made. In a number of tumors the compact cellular areas appeared to arise from proliferating follicular cells. This observation was particularly striking in one neoplasm in which cells tended to pile up, filling follicular lumens, reminiscent of the proliferative alterations observed in thyroids of iodine deficient dogs (see Histologic Response of the Canine Thyroid to Iodine Deficiency) (Figure 25). A cribriform pattern was frequently seen between follicular and compact cellular regions. The slit-like spaces were often empty, but sometimes contained amorphous, lightly PAS-positive material. Cell size and appearance were similar to those described for follicular and compact cellular neoplasms. In some compactly arranged cells it was possible to demonstrate PAS-stained secretory droplets, but this was more common in follicular portions of the neoplasms.

MIXED PAPILLARY–FOLLICULAR CARCINOMA. Only one neoplasm fulfilled criteria consistent with those of papillary carcinoma of the human thyroid.[11] The tumor was unilateral and occupied the majority of the cranial pole of the involved lobe. Grossly, it was firm and multilobulated with a cream-colored and nodular cut surface.

Although no evidence of metastasis was found, capsular and vascular invasion were readily demonstrable. Approximately one-third of the tumor had a papillary arrangement. The remaining portions were composed of either large irregular follicles or cells in a compact pattern. Papillary regions were characterized by long fronds of cuboidal to columnar cells with granular eosinophilic cytoplasm, located upon fibrovascular cores of supporting stroma (Figure 26). Nuclei were sometimes pleomorphic and lacked polarity. Some were vesicular with occasional prominent nucleoli while others approximated the ground glass appearance characteristic of human papillary carcinomas.[40] Psammoma bodies and mitoses were not present.

MEDULLARY CARCINOMA. Both tumors were unilateral and involved the right thyroid lobe. They were firm, about 4 cm in diameter and had nodular external surfaces. The cut surface of one (Case A) was yellow while that of the other (Case B) was cream colored. The neoplasm from Case A was divided into irregular lobules by thick bands of dense, white tissue that coursed through the tumor; the other was lobular on cut

surface but lacked distinct septa. The opposite thyroid lobes appeared grossly normal.

Both neoplasms demonstrated vascular and capsular invasion, but differed histologically. The tumor from Case A was characterized by crisscrossing dense bands of hyalinized connective tissue, usually separating groups of cells into cords or small clusters (Figure 27). In some regions this division was not extensive and larger cellular aggregates were found, as well as a few poorly formed follicles (Figure 28). Throughout this tumor two cell types were seen. Large, polygonal cells (15 to 20 μ) were most abundant. They contained foamy or finely granular cytoplasm and round vesicular nuclei. The second cell type was smaller (5 to 15 μ) and polygonal or fusiform. These cells had brightly eosinophilic, granular cytoplasm and irregular, hyperchromatic nuclei (Figure 28). Mitoses were not present. Immunoperoxidase staining for calcitonin was positive in the majority of tumor cells. Staining intensity varied with stronger reactions, usually in cells with a granular cytoplasm (Figure 27). Silver stains were also positive, but stains for amyloid were negative.

The fine structure of this neoplasm is illustrated in Figure 29. Cells had abundant cytoplasm containing electron-dense round granules. Granules were uniform and measured up to 2500 Å in diameter. They consisted of an electron-dense core surrounded by a limiting membrane. A small amount of well-developed RER was seen, and enlarged saccules suggestive of the Golgi system were found in the vicinity of the nucleus in some cells. Many cells contained abundant cytoplasmic vacuoles. Nuclei were generally oval, with a smooth or wavy outline, and usually contained small nucleoli. Chromatin was finely dispersed with small clumps at the nuclear periphery. Junctional complexes between tumor cells were rare. Collagen fibers were often seen separating cells into small clusters. Typical amyloid fibrils were not seen.

Microscopically, the second medullary carcinoma (Case B) had a compact cellular pattern (Figures 30 and 31, Plate 2). Tumor cells were arranged in lobules of varying sizes and shapes, separated by bands of fibrovascular stroma (Figure 30). Along the periphery of most lobules, cells were columnar and usually lined up perpendicular to the basement membrane (Figures 30 and 31). Toward the center this arrangement was lost, and cells were polygonal (Figure 31). Cells were uniform, measuring approximately 15 μ in diameter, and densely packed, making cytoplasmic borders difficult to discern. Nuclei were round to oval and had a finely stippled basophilic appearance. Nucleoli were not prominent. The cytoplasm was lightly eosinophilic and either granular or finely vacuolated.

Mitotic figures and follicles were not seen. Immunoperoxidase stains for calcitonin were uniformly positive in all neoplastic cells (Plate 2). The palisaded cells at the periphery of lobules generally reacted more strongly than those with a more vacuolated appearance. Silver stains were positive, but like the previously described medullary neoplasm, those for amyloid were negative. The opposite thyroid lobe contained foci of hyperplastic parafollicular cells dispersed among and within thyroid follicles.

ANAPLASTIC CARCINOMA.

1. *Spindle cell carcinoma.* The specimen was from a unilateral resection. The ipsilateral retropharyngeal lymph node was also biopsied. The neoplasm measured 6 cm in diameter, was firm, and had a homogeneous cream-colored cut surface. Microscopically, neoplastic cells were predominantly arranged in small, poorly defined lobules, reminiscent of the pattern seen in compact cellular carcinomas (Figure 32). Follicles were rare. The majority of cells were spindle shaped; however, in a few areas polygonal forms were also seen. Nuclear pleomorphism was striking in some cells. A few nuclei were oval and vesicular, and they measured 12 μ, while most tended to be smaller, hyperchromatic, and fusiform. In some regions, abnormal mitotic figures were numerous. The cytoplasm of most cells was scant and stained lightly eosinophilic. Metastases in the resected lymph node were microscopically similar to the primary tumor.

2. *Giant cell carcinoma.* Both neoplasms were from autopsied dogs and measured 8 cm in diameter. The first contained alternating soft brown and firm cream-colored areas. Microscopically, it was composed of sheets of round and fusiform cells (Figure 33). Follicles were not present. In several areas mutinucleated giant cells, greater than 40 μ, were evident. These cells appeared similar to those described in human tumors of this type [41] (Figure 33). The nuclei of most of the mononuclear and multinuclear cells were vesicular, round, or oval and frequently contained prominent nucleoli. Mitoses were common in many regions. Metastasis to the retropharyngeal and deep cervical lymph nodes was detected, and these metastatic foci appeared similar to the primary neoplasm.

The second neplasm was a firm, irregularly mottled white-gray mass. When the tumor was cut, hard gritty material was encountered. Local extension into the sternocephalic muscles, carotid sheath, right lateral surface of the esophagus were found in addition to multiple firm nodules in the lungs. Microscopically, the neoplasm contained elements of both osteogenic sarcoma and thyroid carcinoma. The sarcomatous portions predominated and were composed of mixtures of fusiform, multinucleate, and stellate cells (Figures 34 and 35). In several areas, fusiform cells

formed spicules of poorly mineralized woven bone. Multinucleate cells, resembling osteoclasts, were frequent adjacent to boney spicules. Prominent mitotic activity and pleomorphic nuclei were common in sarcomatous portions of the tumor. The carcinomatous foci consisted of islands of uniform epithelial cells surrounded by whorls of fusiform cells (Figure 35). These cells had scant amounts of cytoplasm and round to oval vesicular nuclei with prominent nucleoli. For the most part, cells were compactly arranged, but occasionally microfollicular structures were seen (Figure 35). Areas of local invasion and lung metastases contained foci identical to the sarcomatous portions of the primary neoplasm; carcinomatous areas were not detected.

3. *Diffuse small cell carcinoma.* This unilateral tumor was obtained at autopsy. Grossly, it was firm, mottled red and tan, and adherent to the esophagus. The lungs contained soft tan nodules, as did the kidneys, right adrenal, mesentery, and diaphragm. Microscopically, the neoplasm was composed of loosely aggregated uniform, small, round 5- to 10-μ cells with oval, vesicular nuclei and scant amounts of cytoplasm (Figure 36). Mitoses were rare. In a few regions these cells formed structures resembling follicles (Figure 37). Metastatic lesions appeared identical to the primary neoplasm.

SECONDARY CARCINOMA. The thyroid glands of dogs are rarely sites of metastasis or local invasion by other primary neoplasms. In the present study, three such examples were found. Two were primary adenocarcinomas of the lung, while the other was a squamous cell carcinoma arising in the crypt of the pharyngeal tonsil. The pattern of growth in all three metastatic tumors was clearly distinct from that of a primary carcinoma of the thyroid. Neoplastic cells occurred as multiple emboli within the interfollicular network of small veins and lymphatics (Figure 38).

Ectopic Thyroid Tumors of Dogs. In dogs, ectopic thyroid tissues are frequently found in fatty masses adjacent to the ventrolateral wall of the ascending aorta and in a number of cervical and other thoracic sites.[36,42-47] Knowledge of the location of these tissues is important to the oncologist because spontaneous neoplasms found at the base of the heart are not uncommon in this species.[48-52] Histologically similar tumors may originate in the same location from either paraganglia or ectopic thyroid tissue, thus posing a problem in distinguishing between them. Thake *et al.*[53] and Cheville [54] have studied and compared the ultrastructure and histochemical features of ectopic canine thyroid tumors and paragangliomas located at the base of the heart. Ectopic thyroid neoplasms contained

PAS-staining secretory droplets and dense tubules within cisternae of endoplasmic reticulum, features not present in paragangliomas.

In the present study we used a combination of the following histologic features to distinguish between these two tumors. Follicles, or structures that simulated follicles, were found in most ectopic tumors. However, serial sections were sometimes needed to find them. Variations in cell size and shape were common in paragangliomas, while cells in ectopic thyroid tumors were generally more uniform. Tumors originating from ectopic thyroid tissue contained bright, PAS-stained secretory droplets, while paragangliomas lacked this feature. However, cells arranged in a compact cellular pattern stained less intensely than those forming follicles. An argyrophilic network of fibers surrounding nests of cells was noted in paragangliomas, but was not seen in ectopic thyroid tumors.

Of ten ectopic thyroid tumors, seven were associated with unilateral carcinoma of the primary gland, while in three instances the major thyroids were uninvolved. All ectopic neoplasms occurred either within the pericardial sac or just anterior to the heart (Figure 39). Those unassociated with neoplasms of the primary thyroids were seldom detected in the living animal; however, in several cases the neoplasm was large enough to compress adjacent structures and cause dyspnea or dysphagia.

Grossly, most of the tumors were round to oval masses with smooth to nodular external surfaces loosely attached to adjacent structures. Cut surfaces were mottled tan and cream colored, with soft, red necrotic foci. In 2 cases, neoplasms contained multiloculated cysts filled with a mucoid material.

Except for one follicular tumor, all had a mixed follicular–compact cellular pattern (Figures 40 and 41). Several were composed almost entirely of compactly arranged cells, and follicles were rarely found. When present, follicles were either well formed and contained colloid or were less distinct, empty, and resembled microfollicles. PAS-stained secretory droplets were usually demonstrable in cells forming follicles and, to a lesser extent, in compact aggregates. Small blood vessels were usually numerous, and in some neoplasms cells were radially arranged around these structures. Cells comprising most tumors were uniform, cuboidal, or round, with oval, vesicular nuclei, and light, eosinophilic cytoplasm. In the cystic tumors, cells were arranged in sheets and tended to be spindle shaped; in a few areas they formed small follicles that were usually devoid of colloid (Figures 42 and 43). These tumors approximated the appearance of the previously described primary anaplastic (spindle cell) thyroid carcinoma. In both neoplasms, cysts were lined by tall, ciliated

columnar cells, and frequently contained a lightly eosinophilic material with cholesterol clefts that was weakly PAS positive (Figure 42). These structures were considered to be remnants of thyroglossal ducts.

Half of the ectopic neoplasms had histologic features found in malignant tumors. In these cases, neoplastic cells extended into adjacent tissues and/or organs. One tumor, unassociated with carcinoma of the the primary glands, metastasized to the bronchial lymph nodes. Other ectopic neoplasms appeared well encapsulated and were considered to be adenomas.

Five neoplasms were reacted for immunodetectable calcitonin and all were negative. This is in agreement with Kameda's work [47] in which she was unable to find histochemical or ultrastructural evidence for the presence of C cells in nonneoplastic ectopic thyroid tissue of dogs.

Clinical Findings—Feline Cases

General Findings

The majority of benign and malignant thyroid tumors of cats did not produce any clinical signs and were incidental findings at autopsy. However, in 5 cats, benign tumors were large enough to be detected in the living animal, and in 2 instances carcinomas metastasized to regional lymph nodes and caused signs prior to the animal's death. In retrospect, some cats with neoplasms of the thyroid had clinical signs which may have reflected an altered hormonal status, but precise documentation was not available. A PBI determination was done in 1 animal with signs consistent with thyrotoxicosis, and the value was higher (6.0 μg%) than those reported for normal cats.[32]

Classification and Description of Feline Thyroid Tumors

Two entities posed problems in classifying tumors of the feline thyroid. The first was the small, multifocal nodules frequently observed in thyroids of aged cats. These lesions were histologically similar to adenomatous goiters (nodular hyperplasia, nontoxic nodular goiter, or multiple adenomatous goiter) of humans.[10,12] In contrast, the foci in feline thyroids were generally microscopic and rarely caused gross enlargement or distortion of the affected lobules. Although the term *goiter* connotes macroscopic enlargement of the gland, we used it because of the histologic resemblance of the feline thyroid lesion to that occurring in humans. Clark and Meier [2] recognized this problem and also used microscopic criteria to define goiter in feline thyroids. Lucke [5] restricted the use of the term to include only instances in which thyroids were grossly enlarged. She

classified all other lesions as adenomas, regardless of whether they occurred singly or in multiple nodules.

The second entity presenting difficulty in classification was a small group of tumors (8 cases) with histologic and/or cytologic characteristics often associated with malignancy. All of these neoplasms lacked the critical features of capsular and vascular invasion which would define them as carcinomas, and they were designated *atypical adenomas*. This term was first used by Hazard and Kenyon [55] to describe a series of thyroid neoplasms in humans characterized by histologic and cytologic atypia but lacking capsular and vascular invasion. Recurrence was not demonstrated in any subsequent followups. Since all feline tumors were disclosed at autopsy, it was not possible to obtain similar information which would define their biology. These tumors were thus classified as atypical adenomas strictly on the basis of their histologic resemblance to the entity in humans.

No predilection for either lobe was found for benign or malignant tumors. Bilateral involvement occurred in 13 of 17 cats with adenomatous goiters, 2 of 30 with adenomas, and in 1 of 5 with carcinomas.

Benign Tumors of the Feline Thyroid. MULTINODULAR ADENOMATOUS GOITER. Dramatic enlargement and/or distortion of the involved gland were not seen. The affected gland usually had a finely pebbled surface, but occasionally small focal nodules were observed.

Microscopically, the glands contained variably sized foci composed of irregularly arranged colloid-filled follicles, thus differing from the normal adjacent tissue (Figure 44). These areas were seldom totally encapsulated. The surrounding parenchyma was not usually compressed, but exceptions did occur. In a few cases a microfollicular or compact cellular pattern was observed. Colloid-filled cysts were frequently found adjacent to nodules. Cells were uniform and cuboidal with eosinophilic granular cytoplasm, measured approximately 10 μ, and had basal, round, densely chromatic nuclei. Nucleoli and mitoses were absent. In 1 case, amyloid, in varying amounts and occurring almost exclusively between follicles, was detected in the majority of foci (Figure 45). Unlike the usual adenomatous foci, many cells found within amyloid-bearing nodules were polygonal or teardrop shaped, and often had vesicular nuclei with prominent nucleoli

Table 5—Benign Tumors of the Feline Thyroid

Pattern	No. of neoplasms
Multinodular adenomatous goiter	17
Adenoma	22
Atypical adenoma	8

(Figure 45). Other nodules were relatively free of amyloid and contained more uniform cells arranged in closely packed, irregular follicles or as compact cellular foci. Immunoperoxidase staining of this lesion was negative.

ADENOMA. In contrast to multinodular adenomatous goiters, these tumors enlarged and distorted the affected lobe. Adenomas were solitary, soft tan, and occupied the major portion of a thyroid lobe. Some tumors had a pebbled external appearance and a faintly lobular cut surface. A distinct capsule was seldom present.

Microscopically, adenomas were usually composed of irregularly arranged follicles containing varying amounts of colloid (Figure 46). In a few tumors, papillary infolding of follicular epithelia was prominent, while in others, compact cellular foci were dispersed throughout the affected lobule. Occasionally tumors had a lobular appearance, probably produced by the merging of discrete, partially encapsulated foci (Figure 46). Sometimes this lobular arrangement was less distinct or absent, and neoplasms had a homogeneous appearance. Most tumors occupied the entire lobe and were thus bounded only by the natural capsule of the gland. Cells comprising adenomas were uniform and identical to those found in multinodular adenomatous goiters.

ATYPICAL ADENOMA. In general, these tumors caused enlargement and distortion of the affected lobe. Unlike the typical adenomas, they usually had a smooth capsular surface. The cut surface was frequently homogeneous and cream colored, generally lacking the lobulation seen in some typical adenomas.

Microscopically, atypical adenomas were characterized by foci of closely packed follicles that merged with cells arranged in a compact cellular pattern (Figure 47). In most tumors the transition between these two regions was marked by a cribriform pattern. Follicles were usually devoid of colloid. Calcified intrafollicular concretions were found in one neoplasm. A few neoplasms were separated into indistinct lobules by thin bands of fibrous connective tissue, resembling the arrangement seen in some typical adenomas. Cells of atypical adenomas were larger (10 to 15 μ) than those of typical adenomas (Figure 47). Nuclei were usually round and frequently had distinct nucleoli. The cytoplasm was generally finely granular, but groups of cells with large, singular vacuoles were common in some tumors (Figure 47).

Carcinoma of the Feline Thyroid. FOLLICULAR CARCINOMA. All follicular carcinomas caused enlargement and distortion of the affected lobe. Capsular surfaces were brown and nodular. All contained cystic portions which when cut exuded either a thin, brown fluid or thick, green tenacious

Table 6—Carcinoms of the Feline Thyroid

Pattern	No. of neoplasms
Follicular	4
Papillary	1

material. In two specimens the cyst occupied most of the lobe (Figure 48), while in the others only focal areas were affected. On cut surface the remaining tissue was nodular and cream colored.

Two follicular tumors were well differentiated and closely approximated the histologic arrangement and cytology seen in adenomas (Figures 49 and 50). Both were largely composed of uniform cells arranged in distinct follicles that contained little colloid. In a few areas a compact cellular pattern was found, but this arrangement was not predominant. Nuclear pleomorphism and mitoses were not present in either tumor. A large cystic focus filled with colloid and degenerating cells occurred in one neoplasm. A few laminated calcified intrafollicular concretions were present in the other carcinoma. Foci of lymphocytes were found within the thickened capsule of both tumors. Invasion of capsular vessels was prominent in both neoplasms, and in one, metastasis to the mandibular and retropharyngeal lymph nodes occurred (Figure 50).

The remaining two follicular carcinomas were less differentiated than the others. One was characterized by small, densely arranged follicles, usually devoid of colloid, that merged with cells arranged in compact cellular foci. This tumor had many of the features seen in atypical adenomas, but capsular and vascular invasion were detected. Neoplastic cells appeared larger than those of the two well-differentiated carcinomas but, for the most part, were uniform in size and shape. Mitoses were not observed, and nuclei tended to be round and often contained prominent nucleoli.

In the other neoplasm bands of connective tissue divided the tumor into distinct lobules (Figure 51). The major pattern consisted of large, closely packed irregular follicles that rarely contained colloid. In a few areas the follicular arrangement was replaced by compact cellular foci (Figure 51). Capsular invasion was a striking feature of this tumor, as was squamous metaplasia of several neoplastic follicles (Figure 52). Aggregates of lymphocytes were commonly observed adjacent to invading cells. Laminated calcified intrafollicular concretions were numerous in both the primary tumor and within metastatic foci in regional lymph nodes. Unlike cells in the well-differentiated carcinoma, the cells in this neoplasm were large (12 μ), had eosinophilic cytoplasm, and contained vesicular nuclei with prominent nucleoli. Mitoses were absent.

PAPILLARY CARCINOMA. This tumor was only detected microscopically, as it did not cause gross alteration of the affected lobe. Both thyroid lobes contained multinodular adenomatous goiters. In addition, the right lobe had a papillary carcinoma arising within an adenomatous focus (Figures 53 and 54). Although this tumor was well circumscribed by a dense fibrous tissue, serial sections revealed areas of capsular invasion. The neoplasm was characterized by papillary fronds of fibrovascular connective tissue lined by large, cuboidal neoplastic cells. These cells had an eosinophilic cytoplasm and contained round, vesicular nuclei with prominent nucleoli. Mitoses and psammoma bodies were not present.

Discussion

Tumors of the canine thyroid have been described in numerous case studies and reviews. Early publications dealt mainly with documenting the frequency of thyroid neoplasm in collections of pathology specimens.[56-58] Later studies reported that thyroid tumors were common among dogs living in geographic regions where iodine deficiency was common.[3,34,36,59-61] Similarly, neoplasms of the human thyroid were reported to be frequent in these areas,[59,62,63] but more recent evidence suggests that a low iodine diet may not be causally related to this tumor in humans.[64,65] We are unaware of any work documenting the experimental induction of thyroid neoplasms in dogs made iodine deficient, although this phenomenon has been reported in rats.[66]

From Rijnberk and der Kinderen's data [26] it appears that approximately 20% of dogs with malignant thyroid neoplasms may also be hyperthyroid. Thyrotoxicosis found in conjunction with diffuse hyperplasia of the gland (Grave's disease) has not been reported in dogs. This is completely unlike the situation in humans, where Grave's disease is the most common cause of hyperthyroidism and carcinomas are rarely associated with toxic signs.[67-69] The experimental induction of hyperthyroidism in normal dogs requires the daily administration of large oral doses of dessicated thyroid. Piatnek and Olson [70] reported that the amount required to make a euthyroid dog toxic was in excess of 400 mg/kg daily. Polyuria, a consistent sign of hyperthyroidism in dogs with functioning tumors, was not elicited until the seventh week of continuous daily oral doses of 900 to 1000 mg/kg. The results of Rijnberk's studies [7] show that thyrotoxicosis may be associated with elevations in circulating HI (largely thyroxine) in some dogs, while in others it probably results from increases in circulating triiodothyronine (T3), not measured by his techniques. Hollander *et al.*[71] have described cases of T3 toxicosis in humans, and Sung and Cavalieri [72] recently documented a case caused by a metastatic thyroid carcinoma.

Medullary carcinoma of the thyroid arises from parafollicular (C) cells and in humans is usually associated with excess secretion of calcitonin.[73] It has been estimated that the tumor comprises 5 to 10% of all malignancies of the human thyroid.[74] The neoplasm may occur sporadically or in kindreds where it has been associated with bilateral pheochromocytoma,[30,75] adenoma of the parathyroid glands,[30,76] multiple mucosal neuromas, and marfanoid features.[77] It is currently thought that since these tissues are derived embryologically from the neural crest, the medullary carcinoma syndrome may result from a defect in precursor cells.[30]

Multiple endocrine neoplasia syndromes similar to those described in humans have been reported in albino rats [78] and old bulls.[79] Boorman *et al.*[80] have documented the frequent occurrence of medullary carcinomas in WAG/Rij rats. Although multiple endocrine neoplasia was common in these animals, no increased association with medullary carcinoma of the thyroid was found.

The most prominent effects of calcitonin are the lowering of serum calcium and phosphorus.[81] Interestingly, although humans with medullary carcinoma have elevated circulating levels of calcitonin, they are not hypocalcemic or hypophosphatemic.[73] In contrast, Young *et al.*[82] reported that when compared with normal control animals, bulls with ultimobranchial neoplasms had slightly lower serum calcium levels. The lowest levels occurred in 2 bulls with the highest calcitonin content in their tumors. In the present study, both dogs with medullary carcinomas were hypocalcemic at some point during the course of their disease. Phosphorus levels were normal in Case A and elevated in Case B. The slightly low level of serum calcium returned to normal following the removal of the neoplasm in Case A; it is therefore possible that the hypocalcemic episode resulted from excess circulating calcitonin secreted by the tumor. In Case B, two contending possibilities seem likely explanations for the lowered serum calcium: a) iatrogenic hypoparathyroidism induced at the time of surgery and b) secretion of calcitonin by undetected metastatic medullary carcinoma. Unfortunately, calcium levels were not obtained prior to surgery, and in the light of subsequent history, neither possibility entirely explains the hypocalcemia. However, hypoparathyroidism would seem the more likely choice.

Diarrhea has been observed in human patients with medullary carcinoma.[31] It is currently believed that this condition may be due to the elaboration of seratonin and/or prostaglandins by the neoplasm.[31] In Case A, diarrhea was the major sign exhibited by the animal. Following removal of the tumor, diarrhea ceased and has not returned. Since other

causes for this sign were not found, it is possible that the condition was due to humoral substances secreted by the tumor.

Williams [83] classified five neoplasms of the canine thyroid as medullary carcinomas strictly on the basis of light microscopy. Since a compact cellular growth pattern, reminiscent of that seen in some medullary carcinomas,[84] is common in canine thyroid neoplasms,[7,9] techniques such as electron microscopy and immunohistochemistry should be used to define the cell of origin. In the present study the medullary carcinoma from Case B closely approximated the histologic pattern seen in compact cellular carcinomas of the canine thyroid. The distinguishing feature of this neoplasm was the pallisading of columnar cells along the periphery of lobules, which was not seen in any of the compact cellular tumors studied. The neoplasm from Case A was also histologically distinct, characterized by collections of polygonal and fusiform cells separated by dense bands of connective tissue. Its fine structure was characterized by the presence of numerous granules, identical to those found in normal parafollicular cells of dogs,[85] pigs,[86] and humans,[87] and in medullary carcinomas of rats [80] and humans.[88] The amyloid stroma characteristic of medullary neoplasms of rats [80] and humans [89] was not present in the canine tumors. Interestingly, hyperplasia of C cells occurred in the nonneoplastic lobe of Case B. Similar changes have been reported to precede medullary carcinomas in humans at risk of developing these tumors.

The present studies show that the proliferative response of the canine thyroid to either iodine deprivation or neoplastic stimuli is often morphologically similar. Both situations are characterized by the filling of follicles with cells that appear functionally and cytologically less differentiated than normal secretory epithelia. The culmination of this process results in the formation of a compact cellular pattern. In thyroids from iodine-deficient dogs the evolution of this pattern is diffuse and orderly, probably due to a regulated cellular response to TSH. In neoplastic glands, growth is haphazard, reflecting the autonomy of the cells. Autoradiographic and ultrastructural studies of compactly arranged neoplastic cells support the contention that they are poorly differentiated follicular cells. While radioiodine was mainly concentrated in follicular portions of a mixed compact cellular carcinoma, the isotope was also taken up in solid area. Compactly arranged cells were devoid of colloid droplets and lacked many of the organelles commonly associated with secretory activity. However, they did contain microtubules which have been described in normal canine follicular cells.[90] These structures are thought to function in the endocytosis and secretion of colloid. Microtubules have

also been described in ectopic follicular adenomas [53] and in a carcinoma of the canine thyroid.[91] Fine structural studies of cells forming microfollicles did not show evidence of secretory activity. Colloid droplets have been demonstrated in microfollicular carcinomas of humans.[92] In contrast to other canine thyroid tumors, the fine structure of neoplastic follicular cells from a hyperthyroid dog was characterized by features associated with marked functional activity, such as numerous colloid droplets, elongated microvilli, and dilated cisternae of RER. These cells had some of the features seen in hyperplastic human thyroid [93] and TSH-stimulated thyroids of dogs,[94] rats,[66,95] and guinea pigs.[96]

Anaplastic carcinomas comprise from 15 to 20% of all malignant neoplasms of the human thyroid.[97] They are uncommon in dogs,[98,99] and unlike the tumors in humans, frequently contain malignant bone or cartilage. Recently, Jao and Gould [100] and Gaal *et al.*[101] have studied the ultrastructure of anaplastic carcinomas of the human thyroid and concluded that they were of follicular epithelial origin.

Little is known about thyroid tumors in domestic cats. Most information comes from surveys of pathology collections [102-104] or scattered case reports.[105,106] Two publications describe the morphology of a series of feline thyroid tumors.[2,5] From available information it appears that benign tumors of the feline thyroid are not uncommon, carcinomas are rare, and both occur almost exclusively in old cats.[2,5,105,106] Of the ten carcinomas reported in these publications, only four had metastases. In the remaining cases, criteria that would define the malignant nature of the tumors were not reported. Amyloid deposition in adenomatous feline thyroids has been previously described.[2,5] As in the present study, Lucke [5] found amyloid only in the thyroid and other body organs were not involved. Amyloid goiter has been reported in humans.[107]

The cause of multinodular adenomatous goiter in cats is unknown. Scott et al.[108] produced hyperplastic thyroids in kittens fed diets deficient in iodine, but did not state whether changes were multifocal or diffuse. In the present study it was not possible to determine the relationship these nodules had to the development of adenomas and carcinomas. Serial sections of some seemingly homogeneous adenomas disclosed a poorly defined lobulation, suggesting that they were formed by merging of adjacent nodules.

References

1. Mulligan RM: Neoplasms of the Dog. Baltimore, Williams and Wilkins Co, 1949
2. Clark ST, Meier H: A clinico-pathological study of thyroid disease in the dog and cat. Zentralbl Veterinaermed [A] 5:17–32, 1958

3. Moulton JE: Tumors in Domestic Animals. Berkeley, University of California Press, 1961
4. Brodey RS, Kelly DF: Thyroid neoplasms in the dog: A clinicopatholgic study of fifty-seven cases. Cancer 22:406–416, 1968
5. Lucke VM: A histological study of thyroid abnormalities in the domestic cat. J Small Anim Pract 5:351–358, 1964
6. Jubb KVF, Kennedy PC: Pathology of Domestic Animals, Second edition, Vol I. New York, Academic Press, 1970
7. Rijnberk A: Iodine metabolism and thyroid disease in the dog. Utrecht, Drukkerij Elinkwijk, 1971
8. Smith HA, Jones TC, Hunt RD: Veterinary Pathology, Fourth edition. Philadelphia, Lea and Febiger, 1972
9. Von Sandersleben J, Hänichen T: III. Tumours of the thyroid gland. Bull WHO 50:35–42, 1974
10. Meissner WA, Warren S: Tumors of the thyroid gland. Atlas of Tumor Pathology, Second series, Fascicle 4. Washington DC, Armed Forces Institute of Pathology, 1969
11. Hazard JB: Neoplasia. The Thyroid: International Academy of Pathology Monograph. Edited by JB Hazard, DE Smith. Baltimore, The Williams and Wilkins Co., 1964, pp 239–255
12. Sommers SC: Endocrine activities of nonendocrine tissue tumors. Endocrine Pathology. Edited by JMB Bloodworth Jr. Baltimore, The Williams and Wilkins Co, 1968, pp 678–705
13. Franssila K: Value of histologic classification of thyroid cancer. Acta Pathol Microbiol Scand [A] 225 (Suppl):1–76, 1971
14. Vickery AL Jr: Autoradiography of the thyroid.[11] pp 207–225
15. Belshaw BE, Becker DV: Necrosis of follicular cells and discharge of thyroidal iodine induced by administering iodide to iodine-deficient dogs. J Clin Endocrinol Metab 36:466–474, 1973
16. Belshaw BE, Cooper TB, Becker DV: The iodine requirement and influence of iodine intake on iodine metabolism and thyroid function in the adult beagle. Endocrinology 96:1280–1291, 1975
17. Luna LG: Manual of Histologic Staining Methods of the Armed Forces Institute of Pathology, Third edition. New York, McGraw-Hill Book Co, 1968, pp 175–176
18. Grimelius L: A silver nitrate stain for alpha-2 cells in human pancreatic islets. Acta Soc Med Ups 73:243–270, 1968
19. Wolfe HJ, Melvin KEW, Cervi-Skinner SJ, Al Saadi AA, Juliar JF, Jackson CE, Tashjian AH Jr: C-cell hyperplasia preceding medullary thyroid carcinoma. N Engl J Med 289:437–441, 1973
20. Cooper CW, Hirsch PF, Toverud SU, Munson PL: An improved method for the biological assay of thyrocalcitonin. Endocrinology 81:610–616, 1967
21. Tashjian AH Jr, Howland BG, Melvin KEW, Hill CS Jr: Immunoassay of human calcitonin: Clinical measurement, relation to serum calcium and studies in patients with medullary carcinoma. N Engl J Med 283:890–895, 1970
22. Reid CF, Pensinger RR, Ferrigan LW, Parkes L: Functioning adenocarcinoma of the thyroid gland in a dog with mitral insufficiency. J Am Vet Radiol Soc 4:36–40, 1963
23. Rijnberk A: Hyperthyroidism in the dog and its treatment with radioactive iodide. Tijdschr Diergeneeskd 91:789–794, 1966
24. Bohn FK: Der Fall eines abnormen Herzebefundes in Verbindung mit Hyperthyrose beim Hund. Kleint Prax 8:228–233, 1967
25. Rijnberk A, Horst CJG van der: Investigations on iodine metabolism of normal and goitrous dogs. Zentralbl Veterinaermed [A] 16:495–508, 1969

26. Rijnberk A, Kinderen PJ der: Toxic thyroid carcinoma in the dog. Acta Endocrinol [Suppl] (Kbh) 138:177, 1969 (abstr)
27. Rall JE, Robbins J, Lewallen CG: The thyroid. The Hormones: Physiology, Chemistry, and Applications, Vol V. Edited by G Pincus, KV Thimann, EB Astwood. New York, Academic Press, 1964, pp 159–439
28. Fabrizio M, Robbins J: Defective thyroglobulin synthesis in an experimental rat thyroid tumor. J Biol Chem 248:2328–2336, 1973
29. Williams ED, Brown CL, Doniach I: Pathological and clinical findings in a series of 67 cases of medullary carcinoma of the thyroid. J Clin Pathol 19:103–113, 1966
30. Melvin KEW, Tashjian AH Jr, Miller HH: Studies in familial (medullary) thyroid carcinoma. Recent Prog Horm Res 28:399–470, 1972
31. Steinfeld CM, Moertel CG, Woolner LB: Diarrhea and medullary carcinoma of the thyroid. Cancer 31:1237–1239, 1973
32. Bustad LK, Fuller JM: Thyroid function in domestic animals. Lab Anim Care 20:561–581, 1970
33. Wolfe HJ, Voelkel EF, Tashjian AH Jr: Distribution of calcitonin-containing cells in the normal adult human thyroid gland: A correlation of morphology with peptide content. J Clin Endocrinol Metab 38:688–694, 1974
34. Marine D: On the occurrence and physiological nature of glandular hyperplasia of the thyroid (dog and sheep); together with remarks on important clinical (human) problems. Johns Hopkins Hosp Bull 18:359–364, 1907
35. Hazard JB, Kenyon R: Encapsulated angioinvasive carcinoma (angioinvasive adenoma) of thyroid gland. Am J Clin Pathol 24:755–766, 1954
36. Davis DJ: Goiter and malignant growth of the thyroid in the dog. Arch Pathol 26:339–347, 1938
37. McClelland RB: Carcinoma of the thyroid: A report of five cases in dogs. J Am Vet Med Assoc 98:38–40, 1941
38. Krook L, Olsson S, Rooney JR: Thyroid carcinoma in the dog: A case of bone-metastasizing thyroid carcinoma simulating hyperparathyroidism. Cornell Vet 50:106–114, 1960
39. Söderström N, Biörklund A: Intranuclear cytoplasmic inclusions in some types of thyroid cancer. Acta Cytol (Balt 17:191–197, 1973
40. Franssila KO: Is the differentiation between papillary and follicular thyroid carcinoma valid? Cancer 32:853–864, 1973
41. Silverberg SG, DeGiorgi LS: Osteoclastoma-like giant cell tumor of the thyroid: Report of a case with prolonged survival following partial excision and radiotherapy. Cancer 31:621–625, 1973
42. Wölfler A: Die Aortendrüse und der Aortenkropf: Eine vorläufige Mittheilung. Wein Med Wochenschr 5:198–199, 1879
43. Swarts JL, Thompson RL: Accessory thyroid tissue within the pericardium of the dog. J Med Res 24:299–308, 1911
44. Cohrs P: Beitrag zur Kenntnis der intraperikardialen akzessorischen Schilddrüsen und Epithelkörperchen beim Hund (Canis familiaris). Berl Tierärztl Wochenschr 46:683–688, 1930
45. Godwin MC: The early development of the thyroid gland in the dog with especial reference to the origin and position of accessory thyroid tissue within the thoracic cavity. Anat Rec 66:233–251, 1936
46. Blessing MH, Zaborsky F: Über den Nachweis von intrathorakalem Schilddrüsengewebe des Hundes mit I^{131}. Frankfurter Z Pathol 75:14–24, 1966
47. Kameda Y: The accessory thyroid glands of the dog around the intrapericardial aorta. Arch Histol Jap 34:375–391, 1972
48. Bloom F: Structure and histogenesis of tumors of the aortic bodies in dogs: With a

consideration of the morphology of the aortic and carotid bodies. Arch Pathol 36:1–12, 1943
49. Stünzi H, Teuscher E: Zur Histogenese der Herzbasisgeschwülste des Hundes. Zentralbl Veterinaermed 1:87–92, 1953
50. Nilsson T: Heart-base tumours in the dog. Acta Pathol Microbiol Scand 37:385–397, 1955
51. Kast A: Herzbasistumoren beim Hund. Zentralbl Veterinaermed 5:459–474, 1958
52. Misdorp W, Elders RAR: Paragangliomen bij mens en hond. Tijdschr Diergeneeskd 90:205–230, 1965
53. Thake DC, Cheville NF, Sharp RK: Ectopic thyroid adenomas at the base of the heart of the dog: Ultrastructural identification of dense tubular structures in endoplasmic reticulum. Vet Pathol 8:421–432, 1971
54. Cheville NF: Ultrastructure of canine carotid body and aortic body tumors: Comparison with tissues of thyroid and parathyroid origin. Vet Pathol 9:166–189, 1972
55. Hazard JB, Kenyon R: Atypical adenoma of the thyroid. Arch Pathol 58:554–563, 1954
56. Sticker A: Über den Krebs der Thiere: Insbesondere über die Empfänglichkeit der verschiedenen Hausthierarten und über die Unterschiede des Thier- und Menschenkrebses. Arch Klin Chir 65:616–696, 1023–1087, 1902
57. Ewald O: Über maligne Hundestrumen nebst Bemerkungen über die sekretorische Tätigkeit der Schilddrüse. Z Krebsforsch 15:85–110, 1915
58. Kammer F: Über die Metastasenverteilung bei primärem Schilddrüsenkarzinom beim Hund. Inaugural Dissertation, Berne, 1924
59. Wegelin C: Malignant disease of the thyroid gland and its relations to goitre in man and animals. Cancer Rev 3:297–313, 1928
60. Schlotthauer CF, McKenney FD, Caylor HD: The incidence of goiter and other lesions of the thyroid gland in dogs of southern Minnesota. J Am Vet Med Assoc 76:811–819, 1930
61. Cotchin E: Neoplasms of the Domesticated Mammals: Review Series No. 4 of the Commonwealth Bureau of Animal Health; Commonwealth Agricultural Bureau. Bucks, England, Farnham Royal, 1956
62. Ciaudo D, Maroun T, Zebouni F, Geagea E: Le goitre au Liban. Sem Hop Paris 24:2502–2507, 1948
63. Wespi HJ, Eggenberger HU: Rückblick und Ausblick nach 30 Jahren Kropfprophylaxe in der Schweiz. Switzerland, Aarau and Herisau, 1954
64. Dorn HF, Cutler SJ: Morbidity From Cancer in the United States. Washington, DC, Public Health Monogr No. 56, 1959
65. Pendergast WJ, Milmore BK, Marcus SC: Thyroid cancer and thyrotoxicosis in the United States: Their relation to endemic goiter. J Chronic Dis 13:22–38, 1961
66. Axelrad AA, Leblond, CP: Induction of thyroid tumors in rats by a low iodine diet. Cancer 8:339–367, 1955
67. Sussman L, Librik L, Clayton GW: Hyperthyroidism attributable to a hyperfunctioning thyroid carcinoma. J Pediatr 72:208–213, 1968
68. Dorta T, Lemarchand-Béraud Th, Burri C: Ein Fall von Schilddrüsenkarzinom mit hyperfunktionierenden Metastasen. Schweiz Med Wochenschr 98:701–704, 1968
69. Pochin EE, Thompson B: Metabolic activity of tumour tissue. Thyroid Cancer, VICC Monograph Series, Vol 12. Edited by CE Hedinger. Berlin, Springer Verlag, 1969, pp 194–204
70. Piatnek DA, Olson RE: Experimental hyperthyroidism in dogs and effect of salivariectomy. Am J Physiol 201:723–728, 1961

71. Hollander CS, Nihei N, Burday SZ, Mitsuma T, Shenkman L, Blum M: Clinical and laboratory observations in cases of triiodothyronine toxicosis confirmed by radioimmunoassay. Lancet 1:609–611, 1972
72. Sung LC, Cavalieri RR: T3 thyrotoxicosis due to metastatic thyroid carcinoma. J Clin Endocrinol Metab 36:215–217, 1973
73. Tashjian AH Jr, Wolfe HJ, Voelkel EF: Human calcitonin: Immunologic assay, cytologic localization and studies on medullary thyroid carcinoma. Am J Med 56:840–849, 1974
74. Hill CS Jr, Ibanez ML, Samaan NA, Ahearn MJ, Clark RL: Medullary (solid) carcinoma of the thyroid gland: An analysis of the M. D. Anderson Hospital experience with patients with the tumor, its special features and its histogenesis. Medicine (Baltimore) 52:141–171, 1973
75. Williams ED: A review of 17 cases of carcinoma of the thyroid and phaeochromocytoma. J Clin Pathol 18:288–292, 1965
76. Keiser HR, Beaven MA, Doppman J, Wells S Jr, Buja LM: Sipple's syndrome: Medullary thyroid carcinoma, pheochromocytoma, and parathyroid disease; studies in a large family. Ann Intern Med 78:561–579, 1973
77. Steiner AL, Goodman AD, Powers SR: Study of a kindred with pheochromocytoma, medullary thyroid carcinoma, hyperparathyroidism and Cushing's disease: Multiple endocrine neoplasia, type 2. Medicine (Baltimore) 47:371–409, 1968
78. Gilbert C, Gillman J: Spontaneous neoplasms in the albino rat. S Afr J Med Sci 23:257–272, 1958
79. Black HE, Capen CC, Young DM: Ultimobranchial thyroid neoplasms in bulls: A syndrome resembling medullary thyroid carcinoma in man. Cancer 32:865–878, 1973
80. Boorman GA, Noord MJ van, Hollander CF: Naturally occurring medullary thyroid carcinoma in the rat. Arch Pathol 94:35–41, 1972
81. Gray TK, Munson PL: Thyrocalcitonin: Evidence for physiological function. Science 166:512–513, 1969
82. Young DM, Capen CC, Black HE: Calcitonin activity in ultimobranchial neoplasms from bulls. Vet Pathol 8:19–27, 1971
83. Williams ED: Histogenesis of medullary carcinoma of the thyroid. J Clin Pathol 19:114–118, 1966
84. Gordon PR, Huvos AG, Strong EW: Medullary carcinoma of the thyroid gland: A clinicopathologic study of 40 cases. Cancer 31:915–924, 1973
85. Tashiro M: Electron microscopic studies of the parafollicular cells in the thyroid gland of the dog. Okajimas Folia Anat Jap 39:191–211, 1964
86. Fetter AW, Capen CC: Ultrastructural evaluation of thyroid parafollicular cells of pigs with naturally occurring atrophic rhinitis. Pathol Vet 7:170–185, 1970
87. Teitelbaum SL, Moore KE, Shieber W: Parafollicular cells in the normal human thyroid. Nature 230:334–335, 1971
88. Hachmeister U, Zimmermann HD: Elektronenmikroskopische Untersuchungen an einem C-Zellencarcinom. Verh Dtsch Ges Pathol 54:371–375, 1970
89. Meyer JS, Hutton WE, Kenny AD: Medullary carcinoma of thyroid gland: Subcellular distribution of calcitonin and relationship between granules and amyloid. Cancer 31:433–441, 1973
90. Dumont JE, Willems C, Van Sande J, Nève, P: Regulation of the release of thyroid hormones: Role of cyclic AMP. Ann NY Acad Sci 185:291–316, 1971
91. Deutschländer N: Ungewöhnliche Tubuli im Endoplasmatischen Retikulum von Schilddrüsentumorzellen. Virchows Arch [Zellpathol] 11:11–18, 1972
92. Tonietti G, Baschieri L, Salabe G: Papillary and microfollicular carcinoma of human thyroid: An ultrastructural study. Arch Pathol 84:601–614, 1967

93. Heimann P: Ultrastructure of human thyroid: A study of normal thyroid, untreated and treated diffuse toxic goiter. Acta Endocrinol (Kbh) 53(Suppl 110):5–102, 1966
94. Tashiro M, Sugiyama S: Electron microscopic studies of the follicle cells in the thyroid gland of the dog. Okajimas Folia Anat Jap 40:131–160, 1964
95. Wetzel BK, Spicer SS, Wollman SH: Changes in fine structure and acid phosphatase localization in rat thyroid cells following thyrotropin administration. J Cell Biol 25:593–618, 1965
96. Ekholm R, Smeds S: On dense bodies and droplets in the follicular cells of the guinea pig thyroid. J Ultrastruct Res 16:71–82, 1966
97. Thomas CG Jr, Buckwalter JA: Poorly differentiated neoplasms of the thyroid gland. Ann Surg 177:632–642, 1973
98. Mason R, Wells HG: On the occurrence of true mixed carcinomatous and sarcomatous tumors (sarco-carcinoma) with report of a mixed carcinoma-chondrosarcoma of the thyroid of a dog. J Cancer Res 13:207–217, 1929
99. Buergelt CD: Mixed thyroid tumors in two dogs. J Am Vet Med Assoc 152:1658–1663, 1968
100. Jao W, Gould VE: Ultrastructure of anaplastic (spindle and giant cell) carcinoma of the thyroid. Cancer 35:1280–1292, 1975
101. Gaal JM, Horvath E, Kovacs K: Ultrastructure of two cases of anaplastic giant cell tumor of the human thyroid gland. Cancer 35:1273–1279, 1975
102. Huguenin B: Du goitre chez les animaux. Bericht über die Internationale Kropfkonferenz in Bern 24–26 August 1927. Bern, Verlag Hans Huber, 1928, pp 82–89
103. Whitehead JE: Neoplasia in the cat. Vet Med Small Anim Clin 62:357–358, 1967
104. Brodey RS: Canine and feline neoplasia. Adv Vet Sci 14:309–354, 1970
105. Holzworth J, Husted P, Wind A: Arterial thrombosis and thyroid carcinoma in a cat. Cornell Vet 45:487–496, 1955
106. Johnson KH, Osborne CA: Adenocarcinoma of the thyroid gland in a cat. J Am Vet Med Assoc 156:906–912, 1970
107. Walker GA: Amyloid goiter. Surg Gynecol Obstet 75:374–378, 1942
108. Scott PP, Greaves JP, Scott MG: Nutrition of the cat. IV. Calcium and iodine deficiency on a meat diet. Br J Nutr 15:35–51, 1961

Acknowledgments

We wish to acknowledge N. Stewart for her valuable help in preparing this manuscript, Dr. G. Sanders for his aid in analyzing the statistical data, and F. McCarthy for taking the light micrographs.

[*Illustrations follow*]

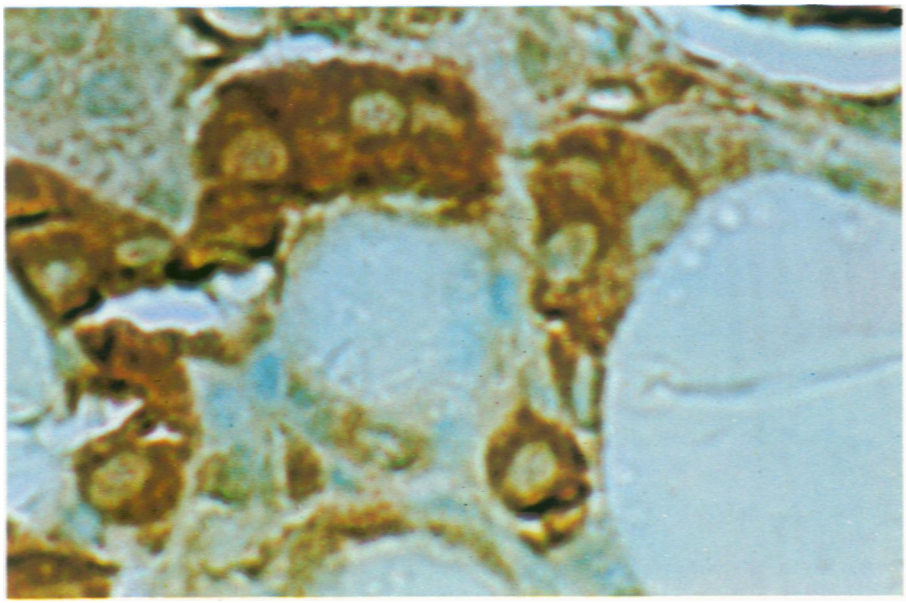

1

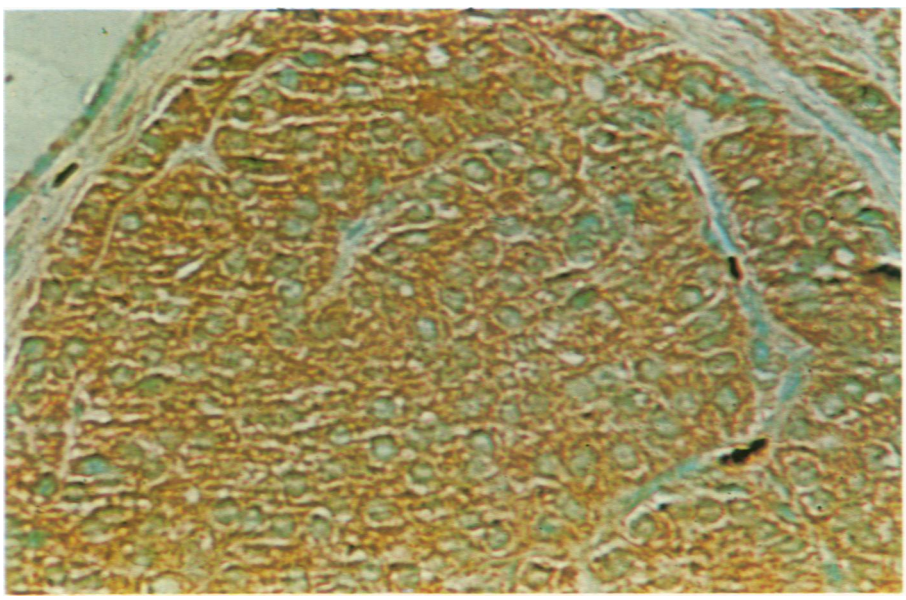

2

Plate 1—Immunoperoxidase reaction for calcitonin in the thyroid of a normal adult male dog. The brown granular reaction product is mainly within cytoplasm of cells between follicles, although a few intrafollicular cells are also present. (Methyl green counterstain, original magnification × 1050). (Courtesy of Drs. H. J. Wolfe and R. A. DeLellis.) **Plate 2**—Immunoperoxidase reaction for calcitonin in a medullary carcinoma of canine thyroid (Case B.) (Methyl green counterstain, × 550). (Courtesy of Drs. H. J. Wolfe and R. A. DeLellis.)

Figure 1—Scintiscan of an 11-year-old male boxer (Category B_{III}) with a mass in the region of the right thyroid lobe. There is faint irregular accumulation of radioactivity in the mass. The contralateral lobe is well visualized. All parameters of iodine metabolism were within normal limits. Microscopically the center of the mass was necrotic. The remaining tissue was a mixed follicular compact cellular carcinoma.

Figure 2—Scintiscan of a 10-year-old German pointer (Category B_{I}) with clinical signs of hyperthyroidism. A small firm mass was palpated in the right cervical region. The *left panel* illustrates the scan prior to the administration of TSH. Autonomous hyperfunction was indicated by the suppressed contralateral left lobe which became clearly visualized subsequent to TSH administration *(right panel)*. Microscopically, the neoplasm was a mixed follicular compact cellular carcinoma.

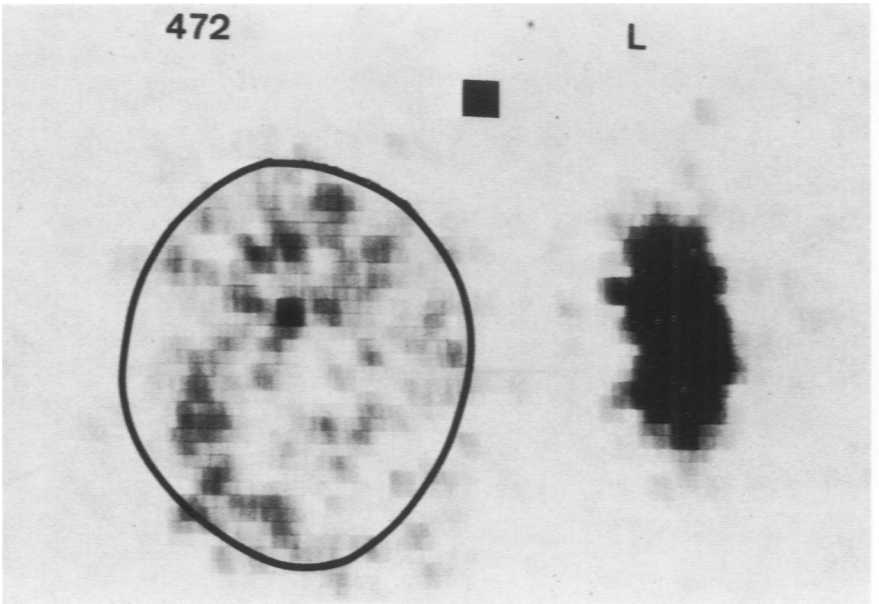

1

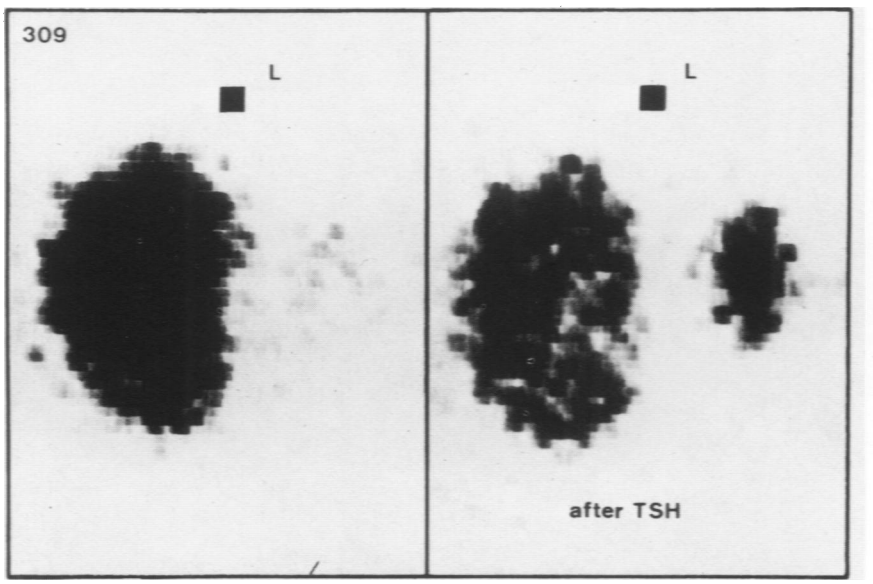

2

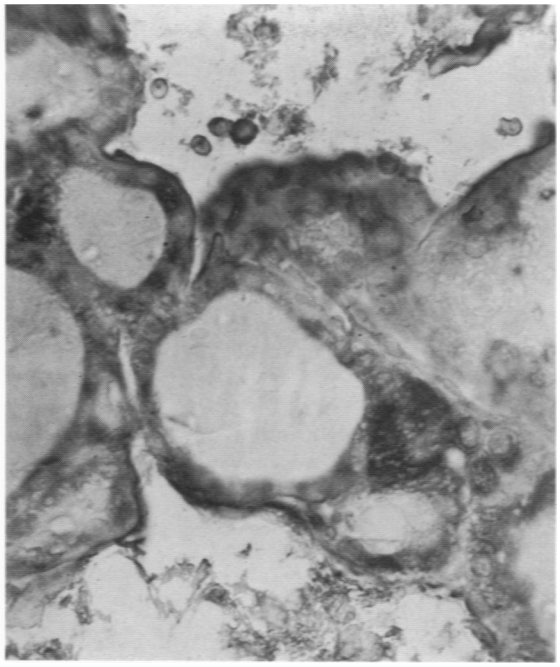

3

Figure 3—Immunoperoxidase reaction for calcitonin in a normal adult male cat. Immunoreactive cells are mainly parafollicular in distribution. The black cytoplasmic granules are immunoreactive sites for calcitonin. (Methyl green counterstain, × 550) (courtesy of Drs. H. J. Wolfe and R. A. DeLellis) **Figure 4**—The effects of iodine deficiency on the canine thyroid. This animal's daily intake of iodine was 44 μg for 8 months. Note the proliferation of follicular cells filling lumens and scalloping of colloid. (PAS, × 670) (courtesy of Dr. B. E. Belshaw)

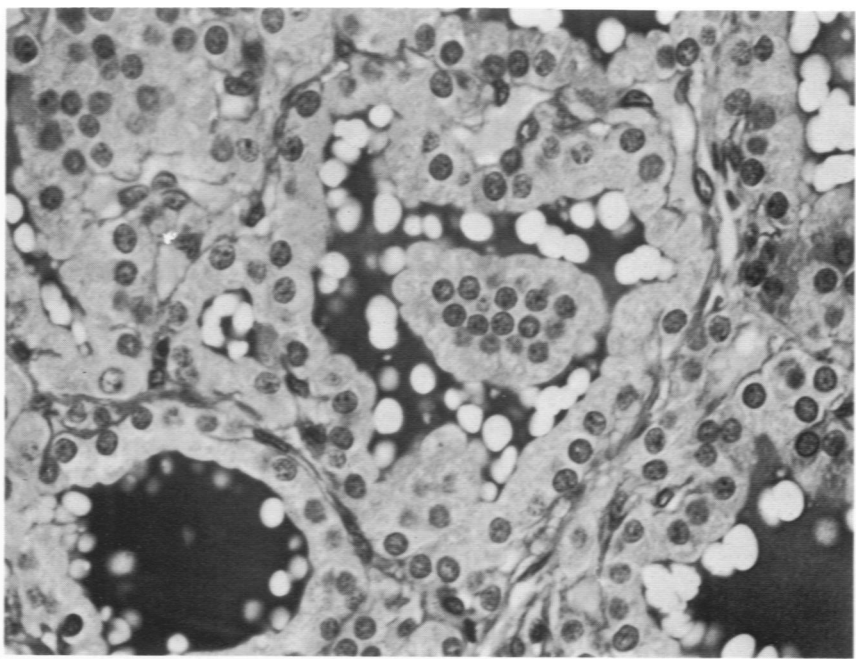

4

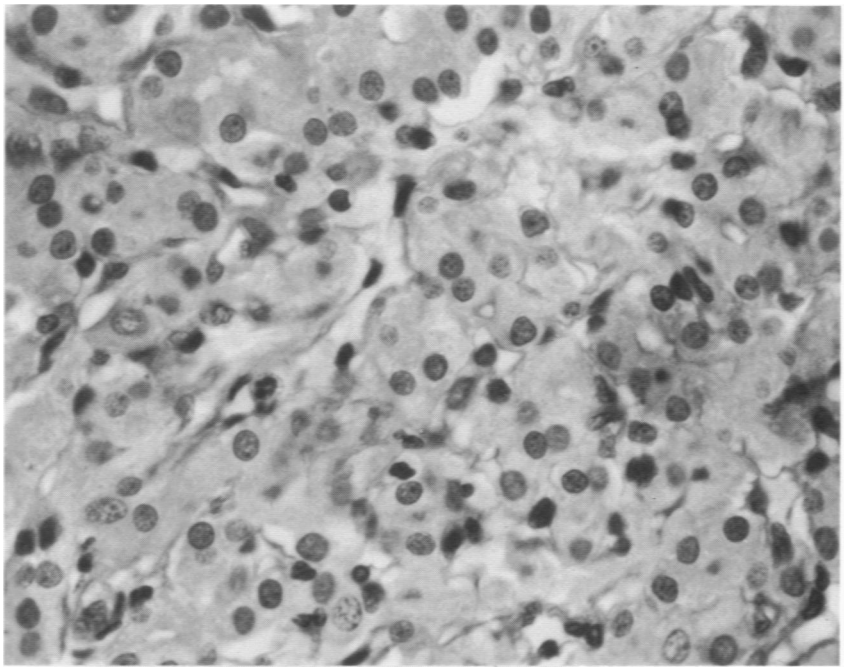

5

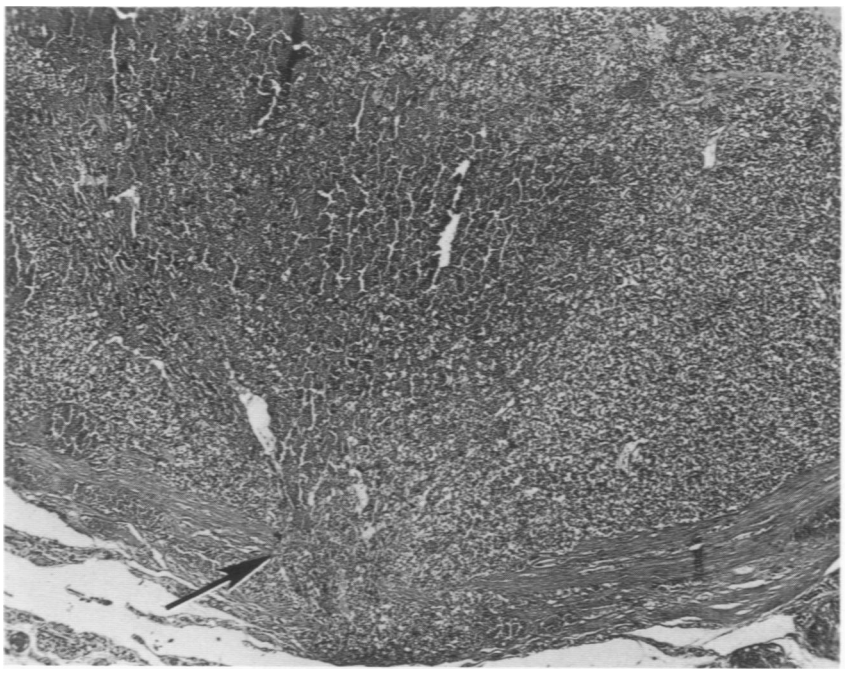

6

Figure 5—This animal's daily iodine intake was 20 μg for 12 months. Follicular lumens are obliterated. The cells are arranged in a compact cellular pattern. (H&E, × 670) (courtesy of Dr. B. E. Belshaw) **Figure 6**—Serial sections of this seemingly well-encapsulated neoplasm revealed evidence capsular invasion (*arrow*) (H&E, × 49).

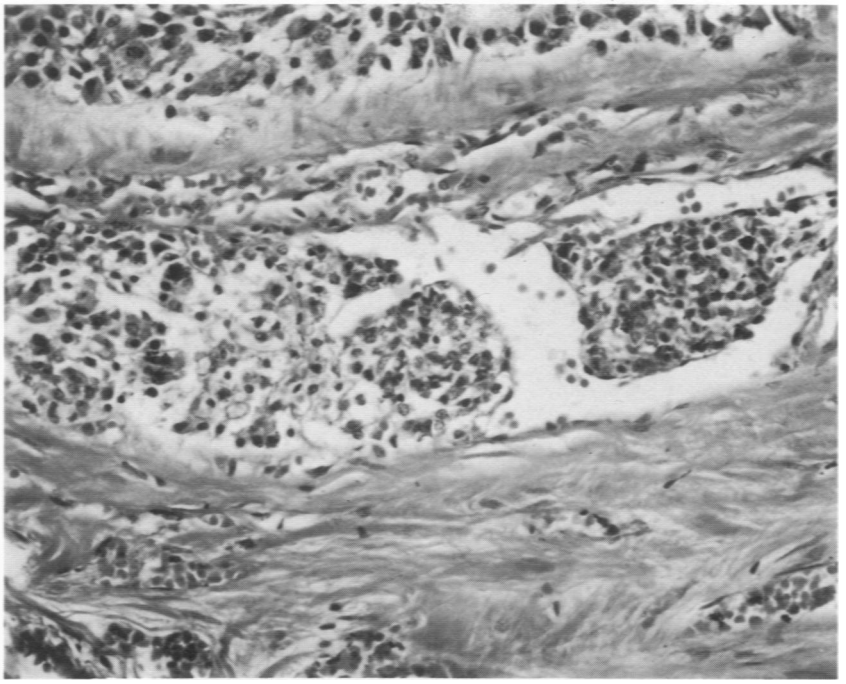

Figure 7—Vascular invasion found after serially sectioning a small seemingly well-encapsulated neoplasm (H&E, × 300). **Figure 8**—Cross section of a locally invasive carcinoma of the canine thyroid. The trachea, esophagus, and carotid vessels have been incorporated into invading neoplasm.

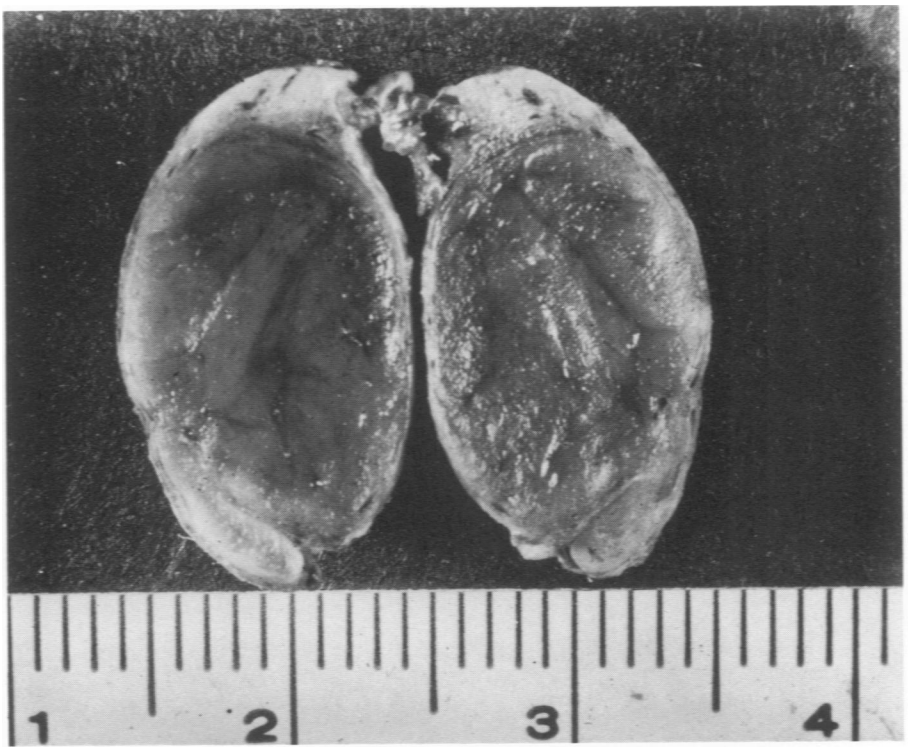

9

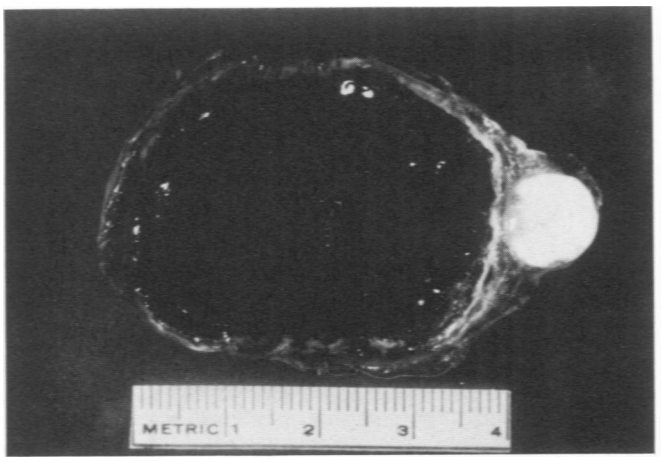

10

Figure 9—Solid adenoma of the canine thyroid, cut surface. The tumor has replaced most of the affected lobe. A thin capsule surrounds the tumor. **Figure 10**—Cut surface of a cystic adenoma of the canine thyroid. When cut, a clear fluid escaped from the central cavity. The cyst is circumscribed by a rugose lining.

11

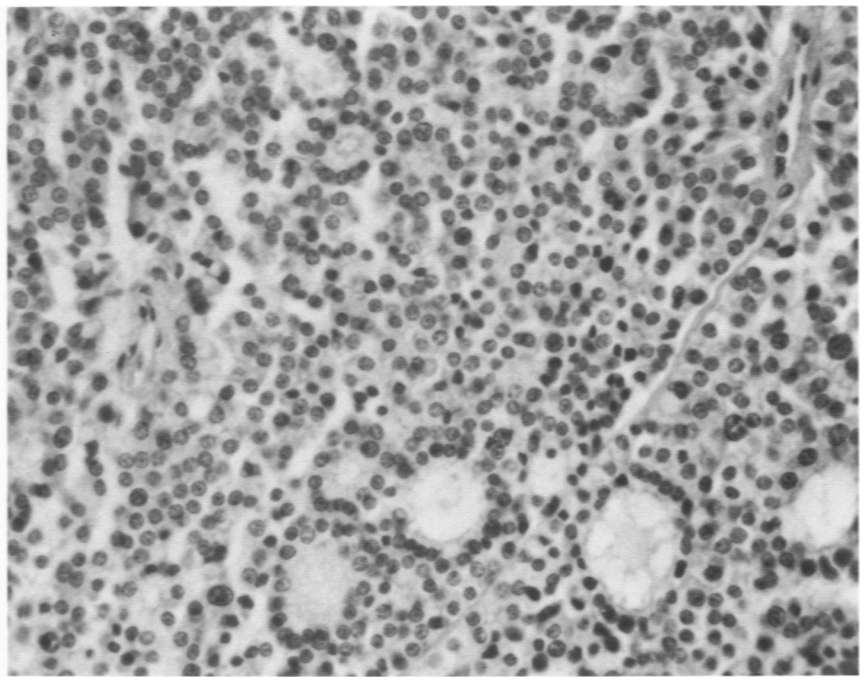

12

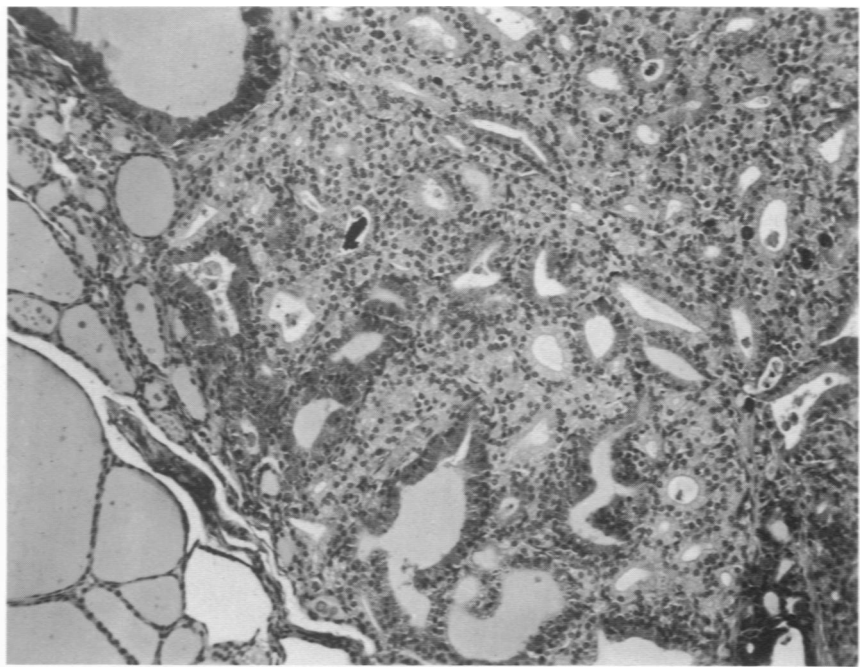

Figure 11—Microfollicular adenoma of the canine thyroid. The neoplasm is characterized by small, poorly formed follicles which vary in shape and content. (H&E, × 500) **Figure 12**—Macrofollicular adenoma of the canine thyroid. The tumor is composed of large irregular follicles. (H&E, × 130)

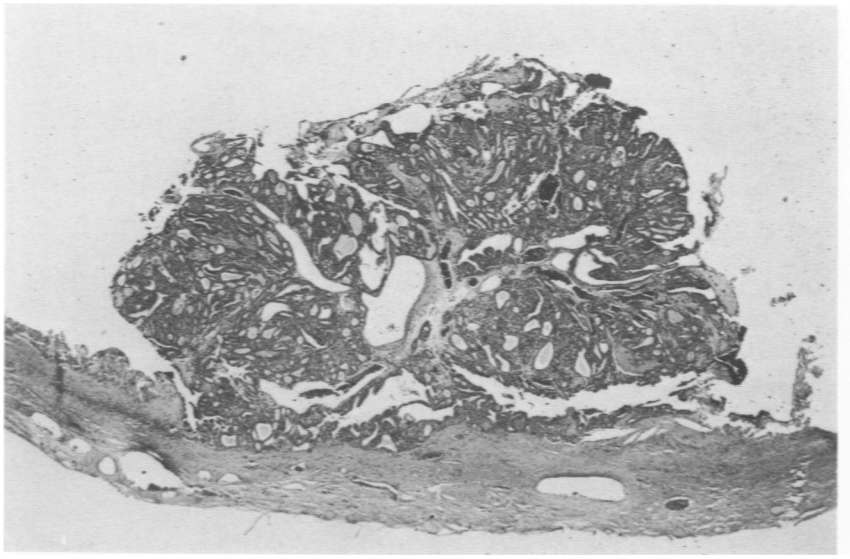

13

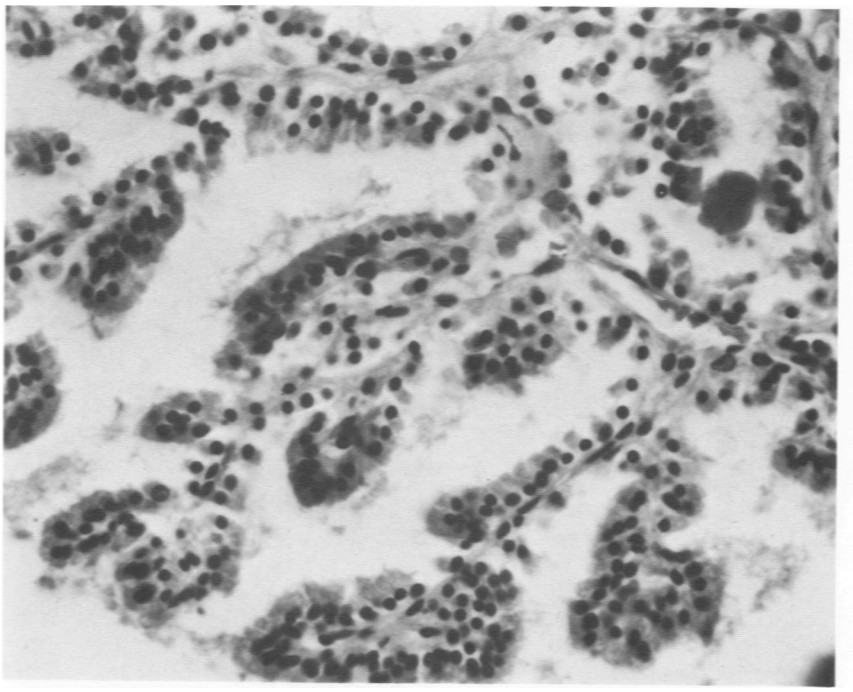

14

Figure 13—Cystic adenoma of the canine thyroid. A mass of irregularly arranged follicles projects from a fibrous connective tissue capsule. (H&E, × 23) **Figure 14**—Papillary adenoma of the canine thyroid. Note the arborescent pattern of the tumor and the uniform appearance of the follicular cells. (H&E, × 500)

15

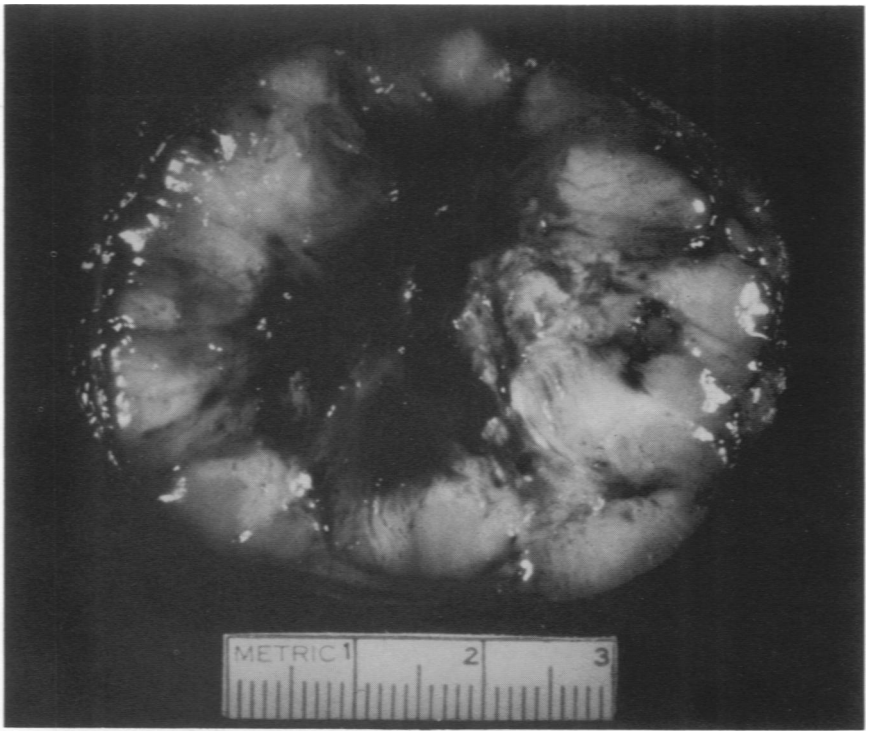

16

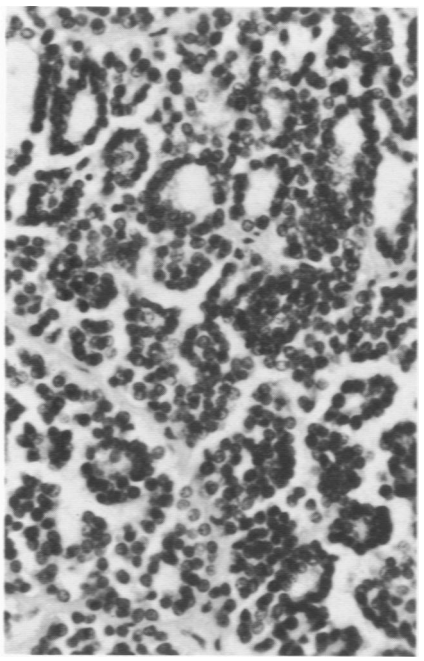

17

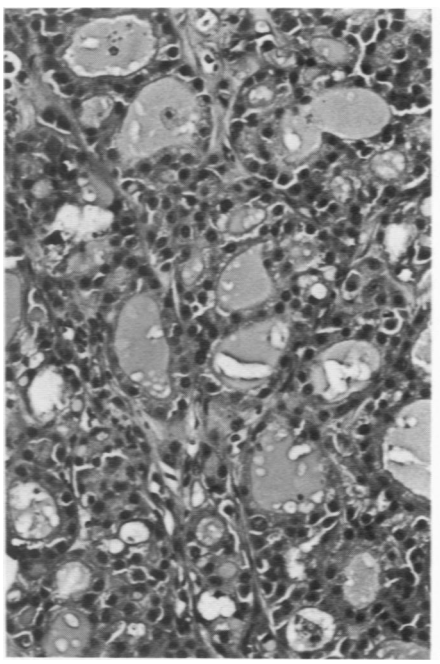

Figure 15—Follicular carcinoma of the canine thyroid. A large necrotic center is common in these neoplasms. **Figure 16**—Follicular carcinoma of the canine thyroid. Most of the neoplastic cells in this tumor formed microfollicles. (H&E, × 360) **Figure 17**—Follicular carcinoma of the canine thyroid. In this neoplasm, cells formed large irregular follicles which frequently contained colloid. (H&E, × 160)

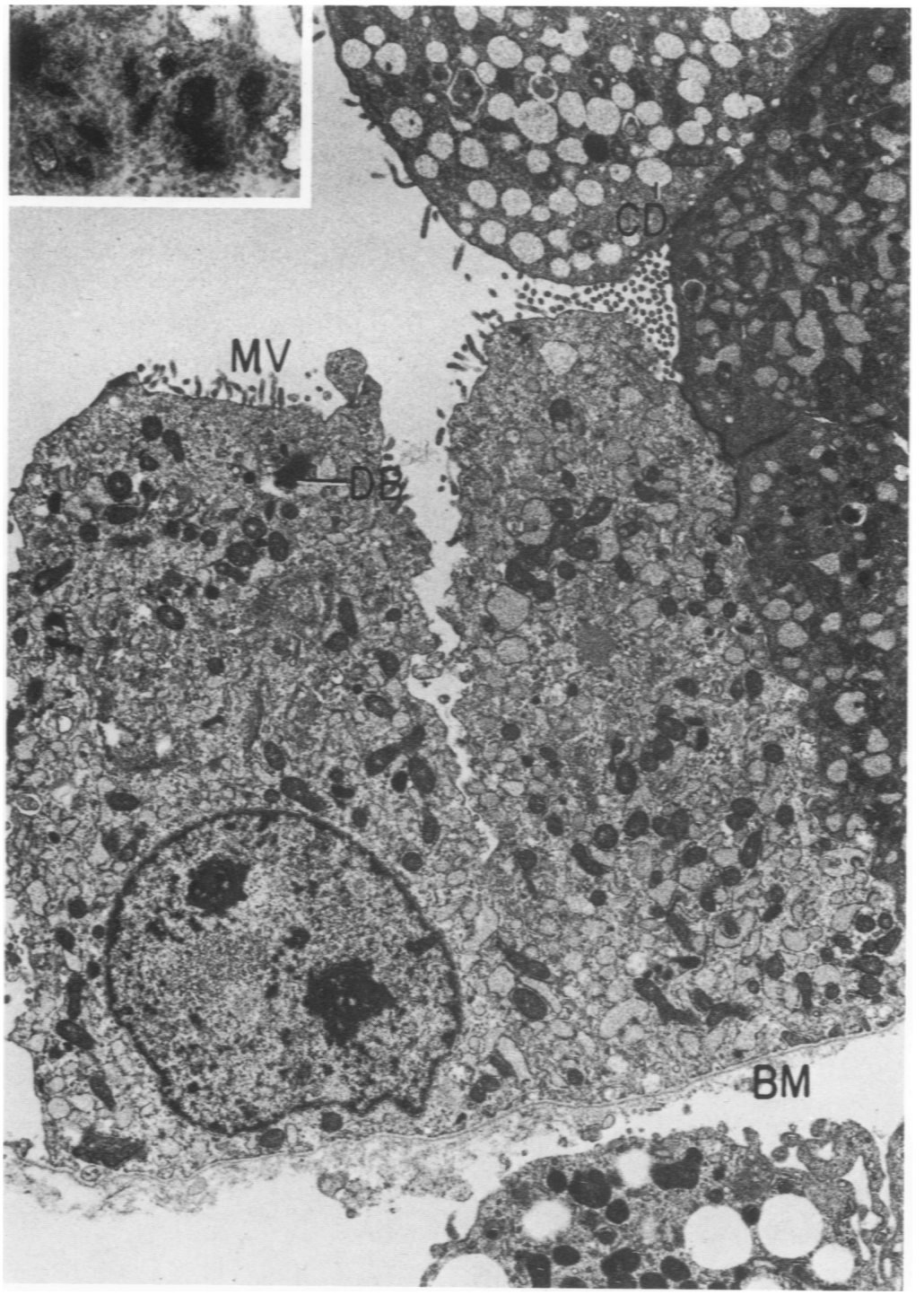

Figure 18—Hyperfunctioning carcinoma of the canine thyroid. The cells are tall columnar with numerous microvilli (*MV*).Colloid droplets (*CD*) are present as are dense bodies (*DB*). The basement membranes (*BM*) are flat. (× 7600) **Inset**—Autoradiograph of this neoplasm. Radiolabeled iodine represented as black granules is present in follicular lumens. (H&E, × 160) (courtesy of Dr. A. Vickery)

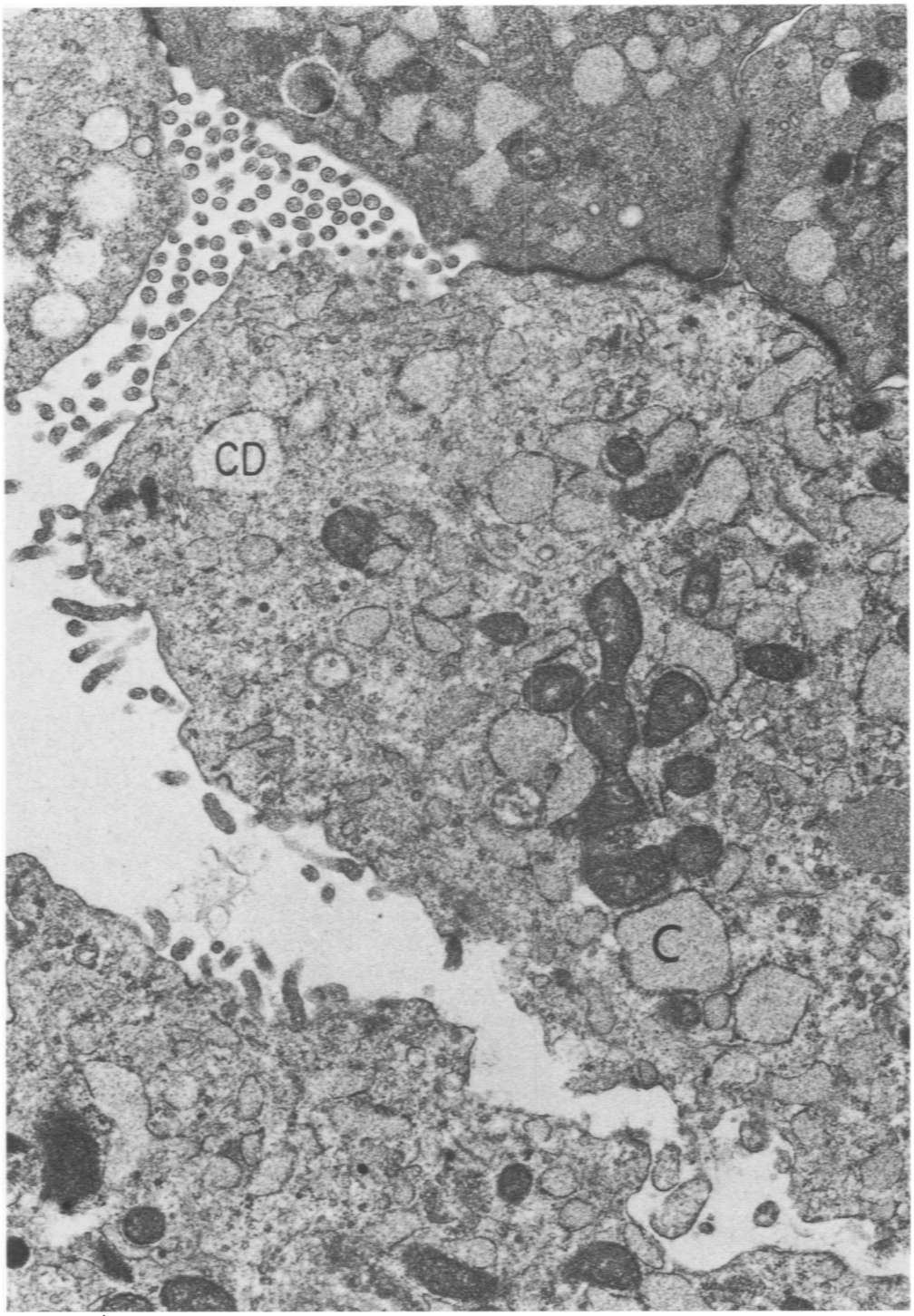

Figure 19—Higher magnification of Figure 18. Note the presence of colloid droplets (*CD*) towards the apices of the hyperfunctioning cells. Increased cellular activity is pronounced as evidenced by dilated cisternae (*C*) of rough endoplasmic reticulum. (× 19,200)

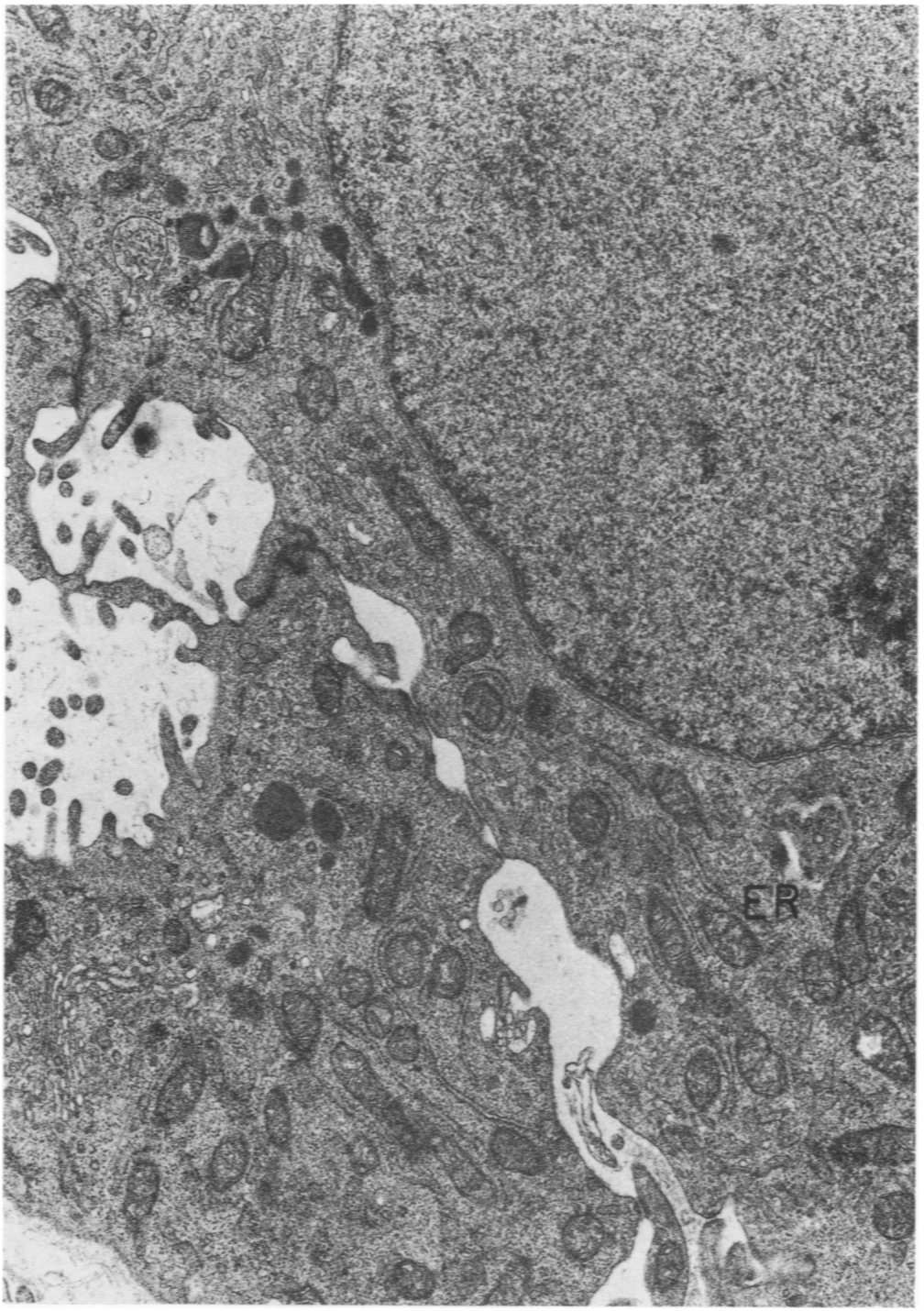

Figure 20—Parts of two cells from a carcinoma in which microfollicules were abundant. Note the presence of microvilli which project into the intercellular space. Free ribosomes and strands of rough endoplasmic reticulum (*ER*) fill the cytoplasm. Although Golgi occurred in some cells evidence of colloid droplets was lacking. (× 19,200)

21

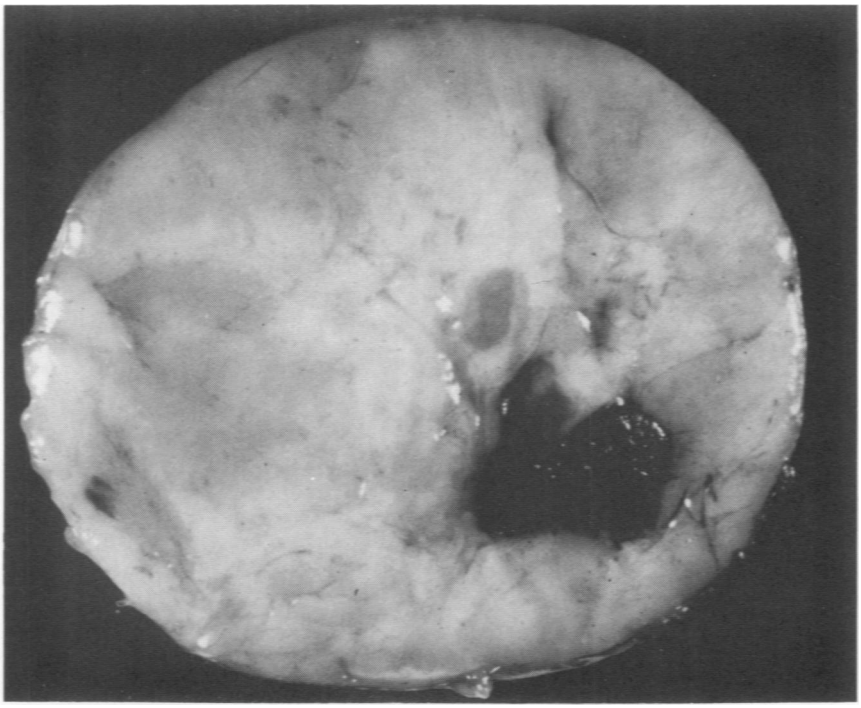

22

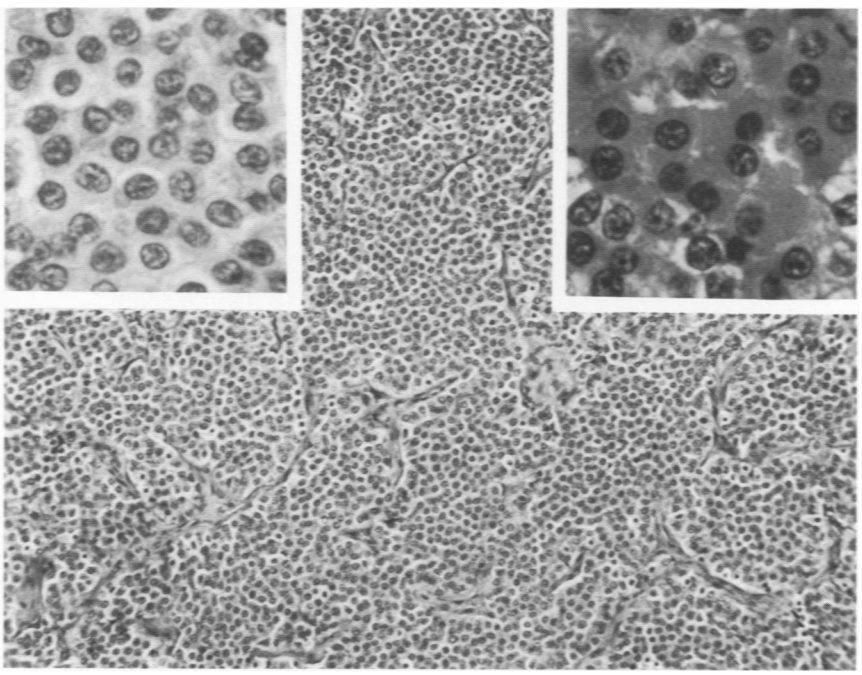

Figure 21—Cut surface of a compact cellular carcinoma of the canine thyroid. The majority of the tumor consists of cream colored finely lobulated tissue. A small eccentric focus of necrotic tissue is present **Figure 22**—Compact cellular carcinoma of the canine thyroid. Sheets of uniform cells are divided by the thin strands of fibrovascular connective tissue. (H&E, × 150) **Inset (right)**—Hurthle cells; Note the dense granular cytoplasm of these cells (H&E, × 580) **Inset (left)**—Higher magnification of compactly arranged cells. The cells are uniform and contain vesicular nuclei. (H&E, × 580)

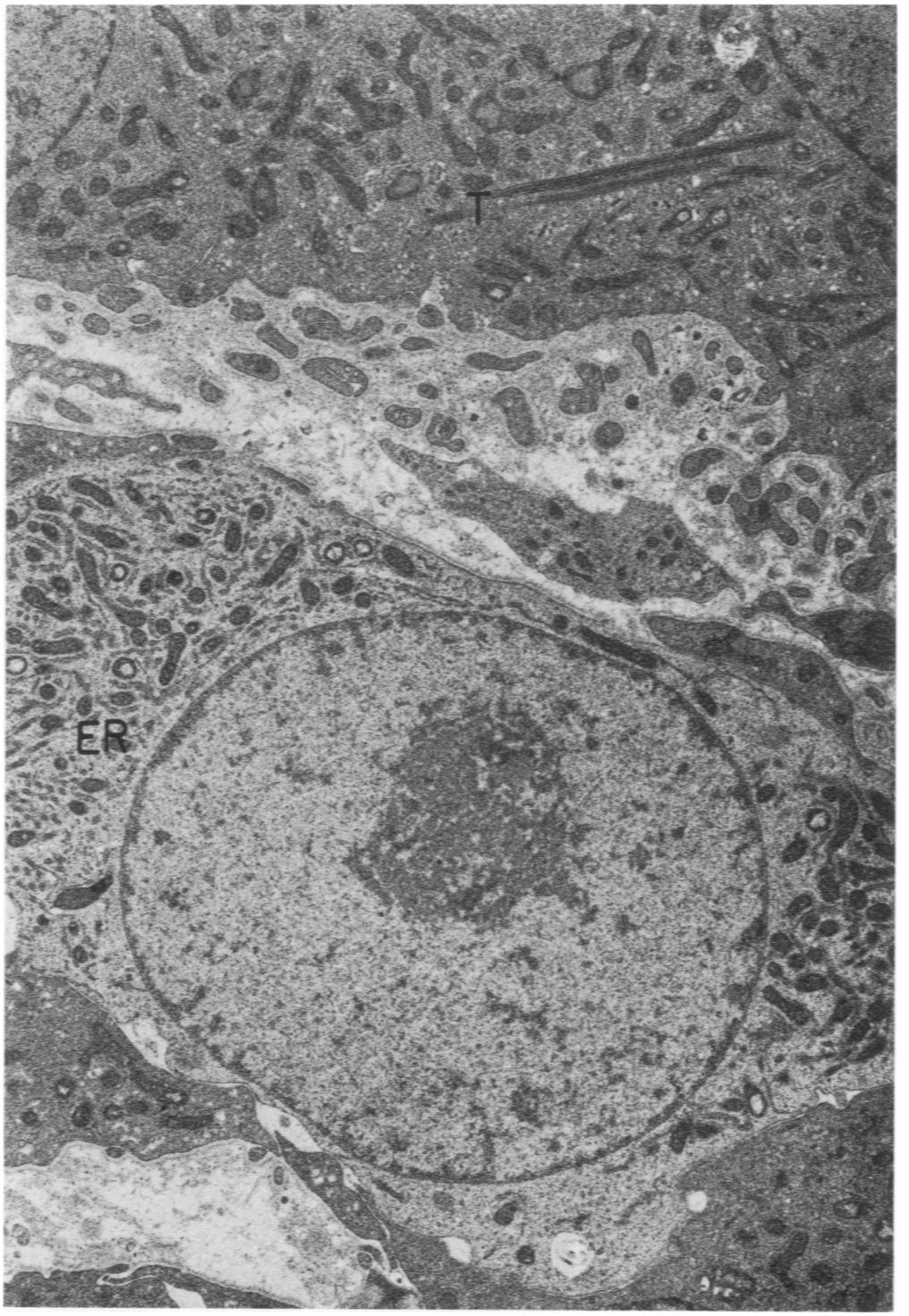

Figure 23—A compact cellular carcinoma of the canine thyroid. The central cell contains fewer free ribosomes than do others in this field and thus stains lighter. Mitochondria and strands of rough endoplasmic reticulum (*ER*) are numerous. Colloid droplets were, however, absent. Note the long tubules (*T*) in the cytoplasm of the cell at the top of the micrograph. (× 9500)

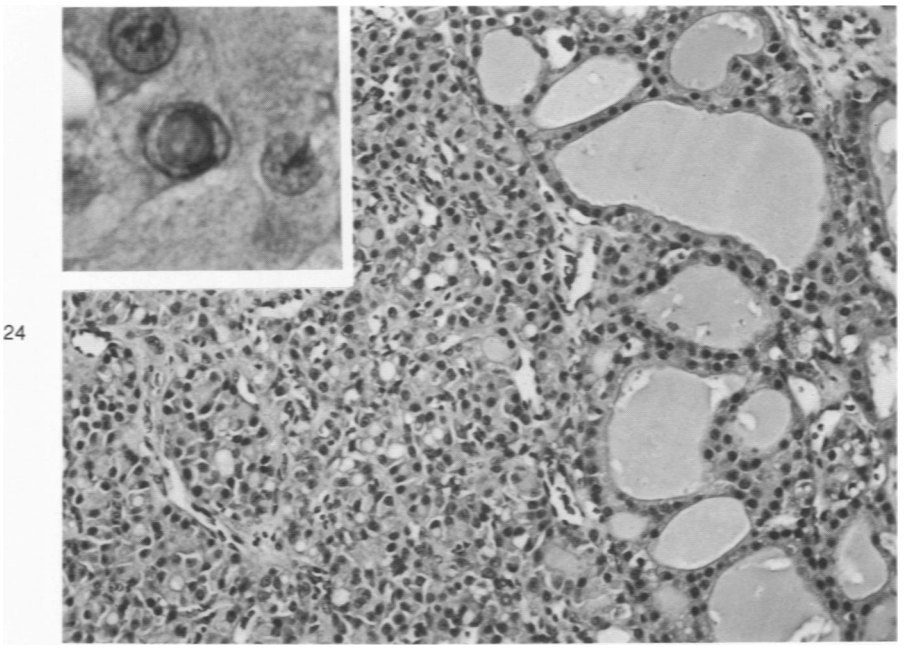

24

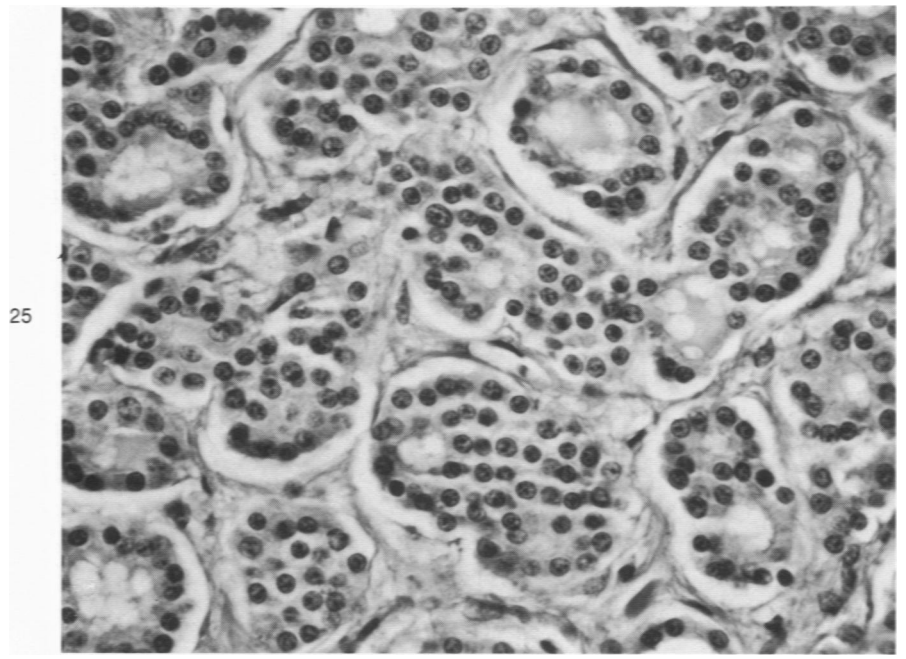

25

Figure 24—Mixed follicular-compact cellular carcinoma of the canine thyroid. Both follicular and compact cellular patterns are evident. (H&E, × 160) **Inset**—Intranuclear inclusion body in a mixed follicular compact cellular neoplasm (H&E, × 950). **Figure 25**—The evolution of a compact cellular pattern, proliferating neoplastic cells fill lumens (H&E, × 500)

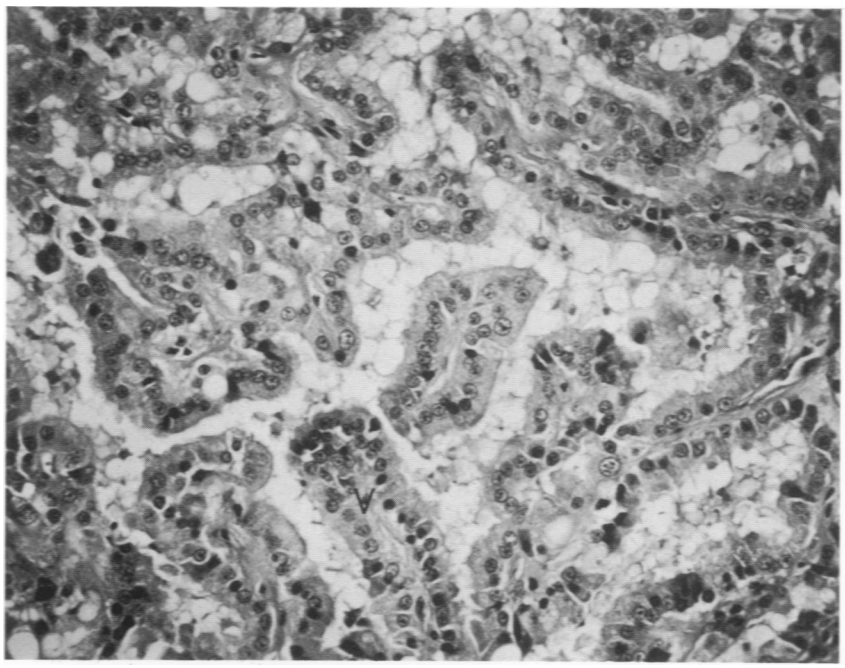

26

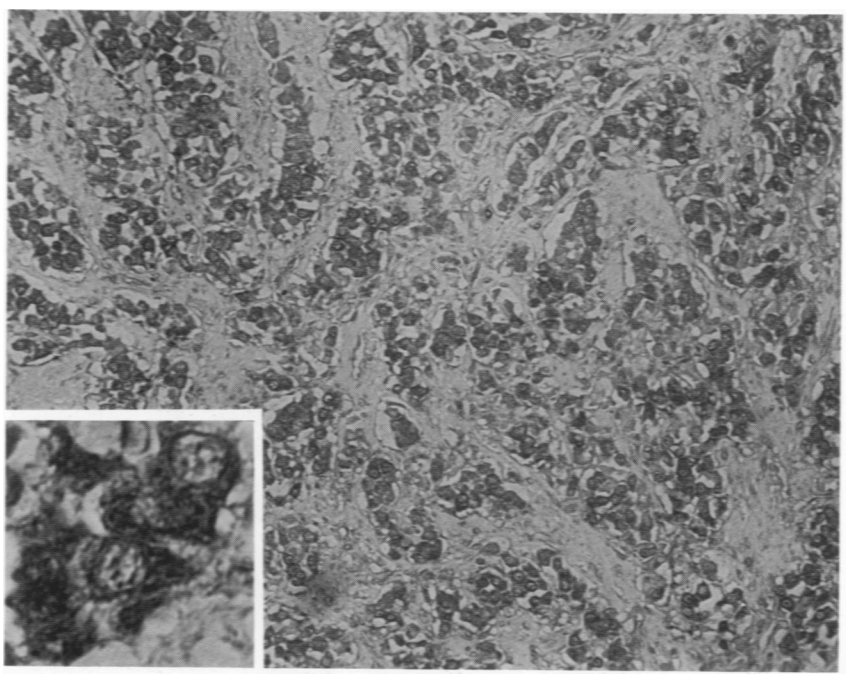

27

Figure 26—Mixed papillary-follicular carcinoma of the canine thyroid. Papillary fronds of fibrovascular tissue bearing neoplastic cells (*V*) project into dilated lumens. (H&E, × 260) **Figure 27**—Medullary carcinoma of the carcinoma of the canine thyroid (Case A). Dense bands of hyalinized tissue surround cords of neoplastic cells. Immunoperoxidase reaction for calcitonin. (× 170) **Inset**—Black cytoplasmic granules represent sites of immunoreactivity. Immunoperoxidase reaction for calcitonin. (× 320) (courtesy of Drs. H. J. Wolfe and R. A. DeLellis)

28

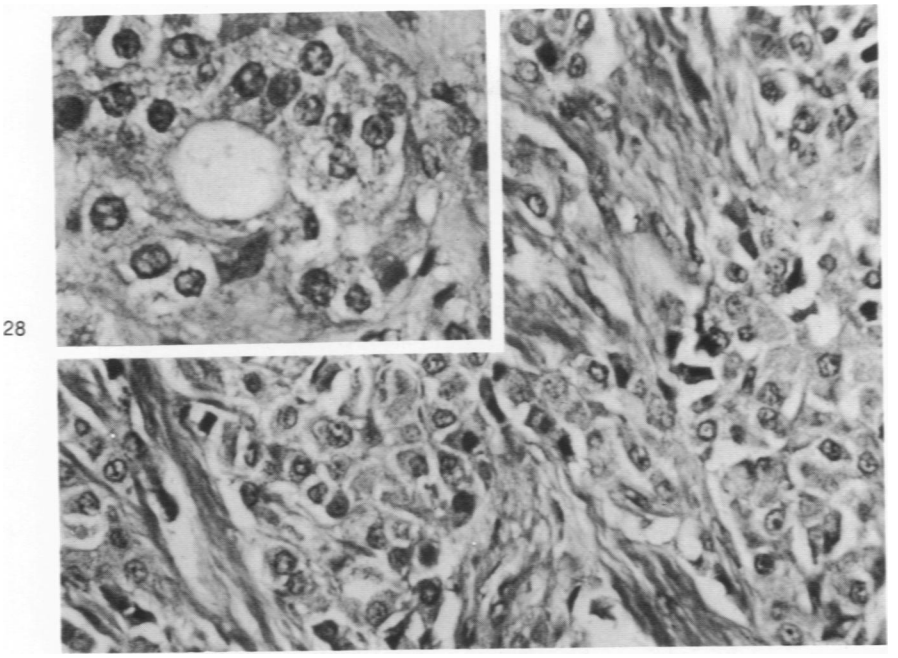

29

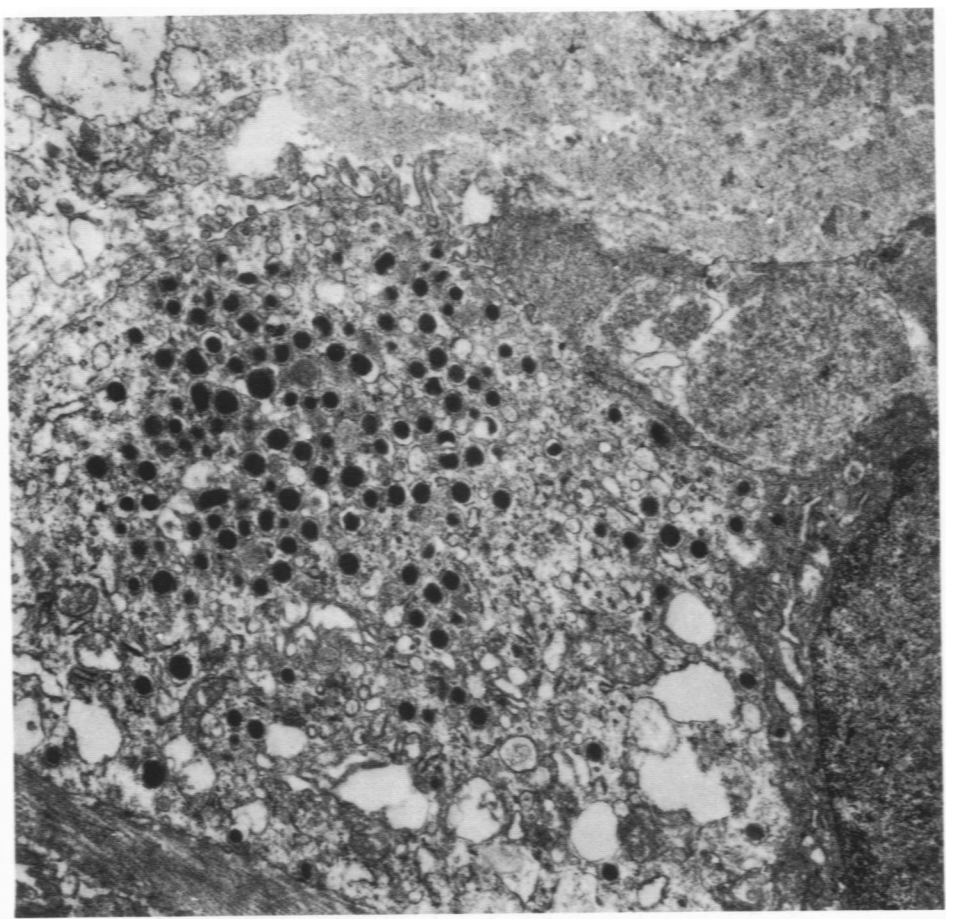

Figure 28—Medullary carcinoma of the canine thyroid (Case A). Neoplastic C cells are either polygonal with vesicular nuclei or fusiform with hyperchromatic nuclei. (H&E, × 380) **Inset**—Follicles were formed by neoplastic C cells in a few areas of this tumor (H&E, × 670). **Figure 29**—Medullary carcinoma of the canine thyroid Case A. Numerous secretory granules are evident. They have an electron dense core and are membrane bound. The apical surface of the cell contains blunt microvilli. Bundles of collagenous connective tissue (lower left corner of the micrograph) were frequently found between neoplastic C cells. (× 4500) (courtesy of Dr. J. E. Van Dijk)

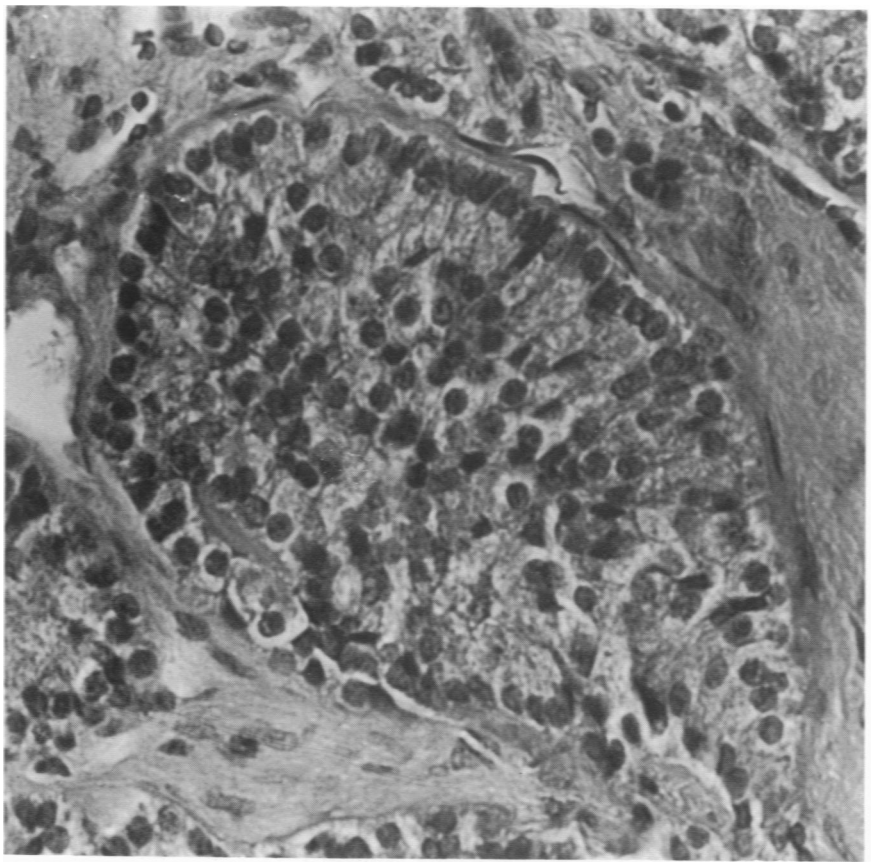

30

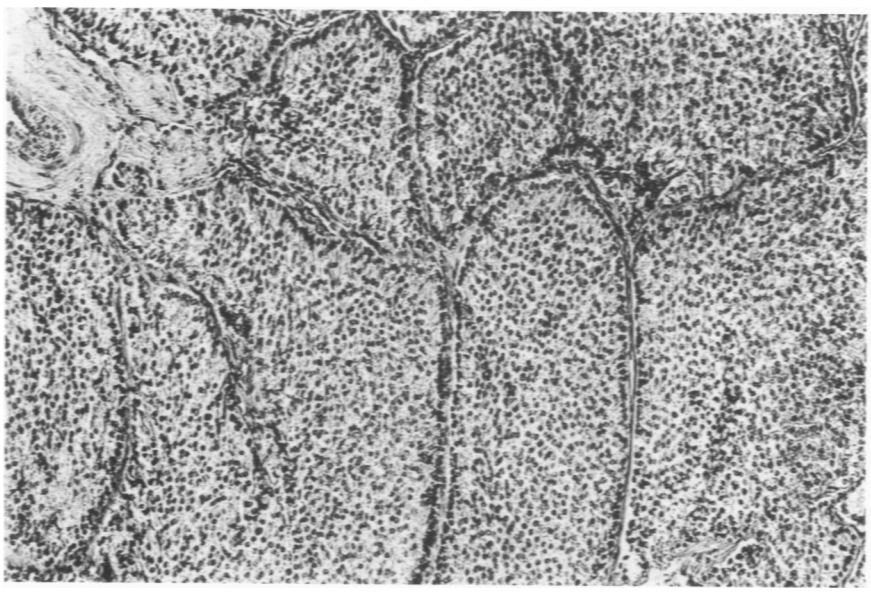

31

Figure 30—Medullary carcinoma of the canine thyroid (Case B). Neoplastic cells are arranged in lobules. Note the palisading of cells along the lobular margins. (H&E, × 120) **Figure 31**—Higher magnification of the medullary carcinoma found in Case B. Cells along the periphery of the lobule are columnar and oriented perpendicular to the basement membrane. (H&E, × 550)

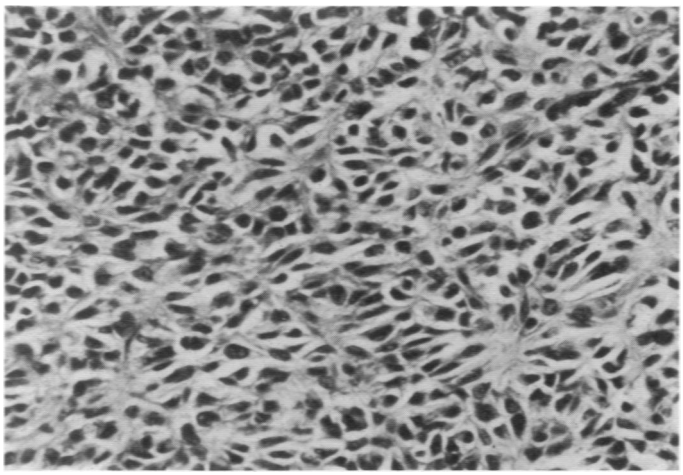

Figure 32—Anaplastic (spindle cell) carcinoma of the canine thyroid. Cells tend to be spindle shaped but are still in packets similar to the arrangement seen in compact cellular carcinomas. (H&E, × 320)

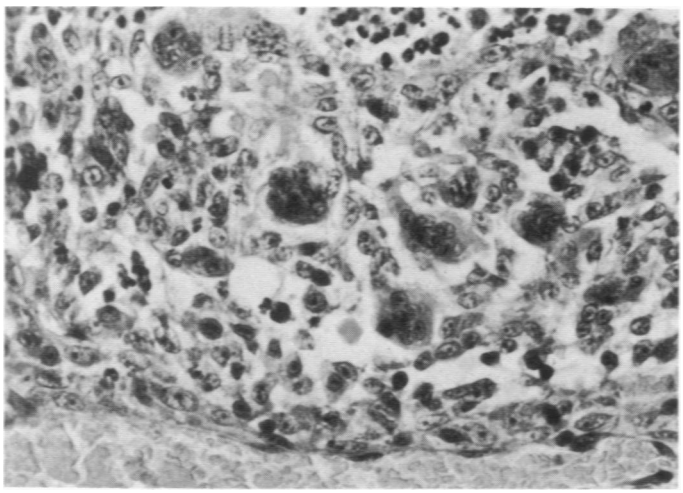

Figure 33—Anaplastic (giant cell) carcinoma of the canine thyroid Cells are round to fusiform and are associated with multinucleate giant cells. (H&E, × 340)

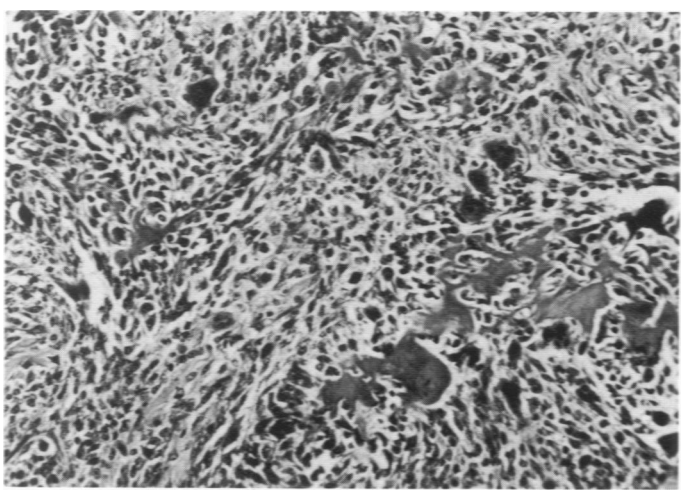

Figure 34—Anaplastic (giant cell) carcinoma of the canine thyroid. This tumor was mainly composed of sarcomatous elements associated with the formation of osteoid and woven bone. Sheets of spindle cells and multinucleate giant cells are seen along with spicules of osteoid. (H&E, ×140)

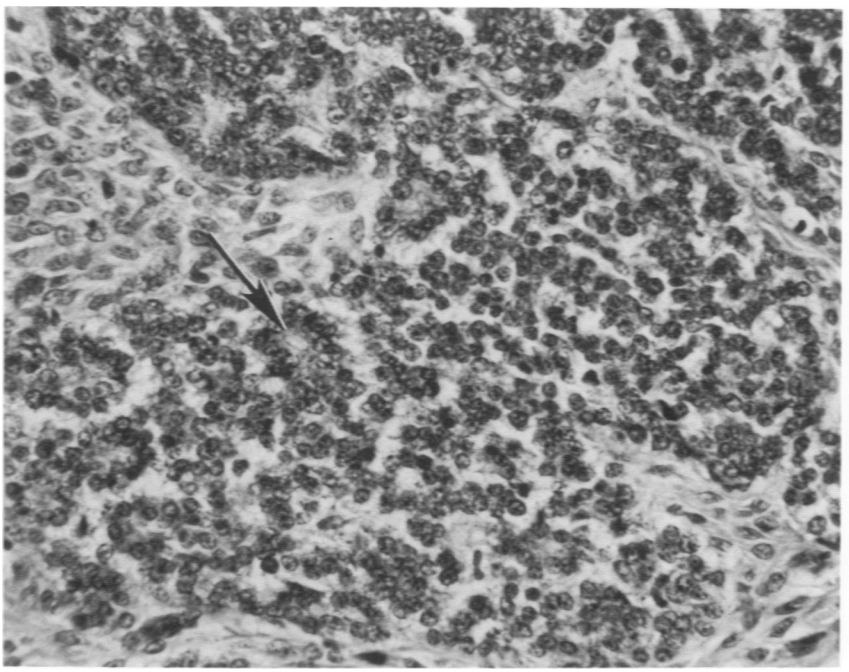

35

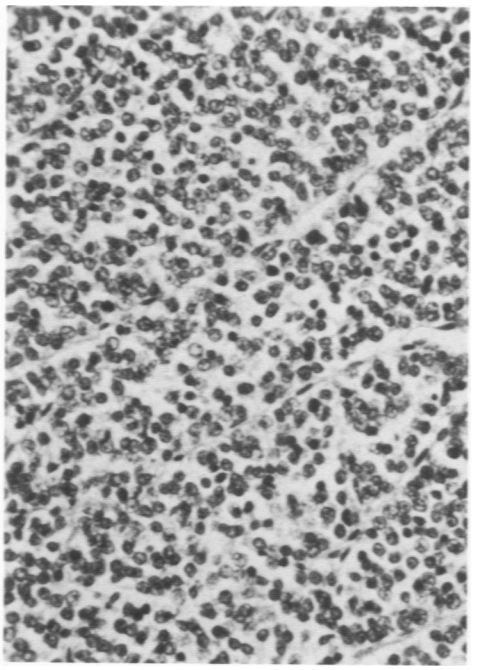

36

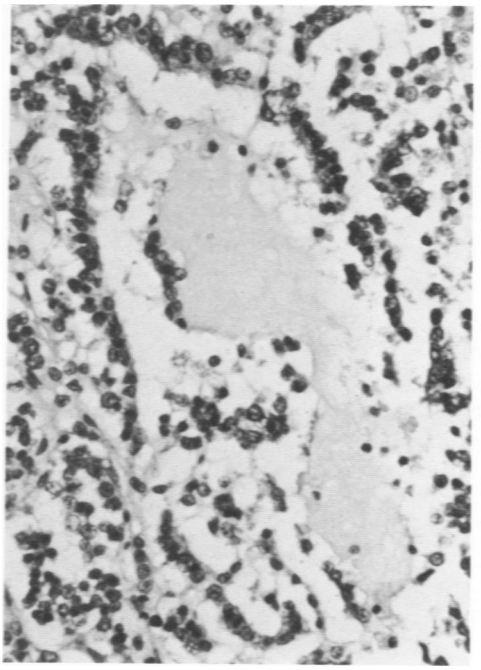

37

Figure 35—Anaplastic (giant cell) carcinoma of the canine thyroid. In some regions of the neoplasm illustrated in Figure 34, cells had an epithelial appearance and formed structures reminiscent of microfollicles (*arrow*). (H&E, × 320) **Figure 36**—Diffuse small cell carcinoma of the canine thyroid. Sheets of cells with round or oval nuclei and scant cytoplasm comprise the tumor. (H&E, ×330) **Figure 37**—Diffuse small cell carcinoma of the canine thyroid. In a few areas of the tumor, structures resembling follicles containing colloid-like material were found. (H&E, × 330)

38

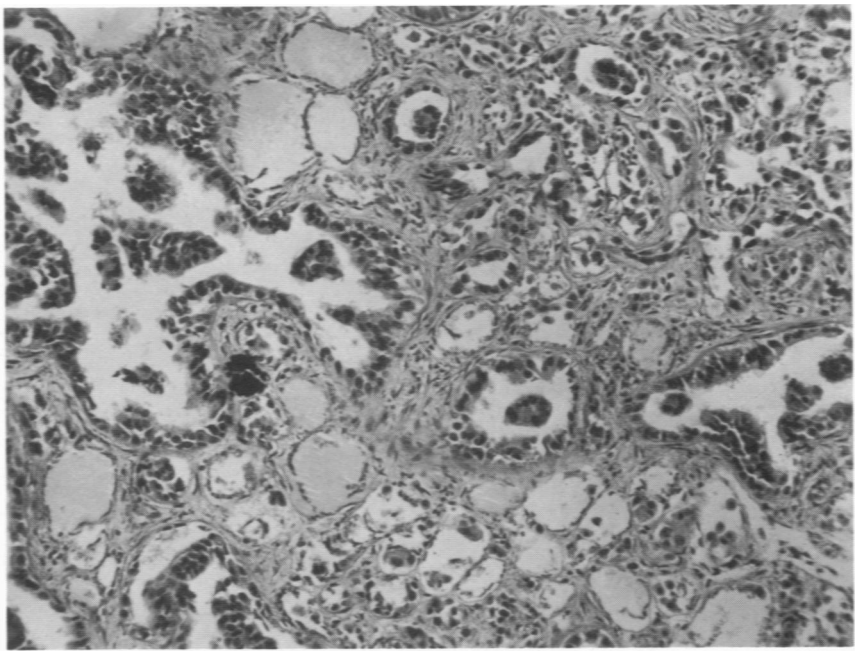

39

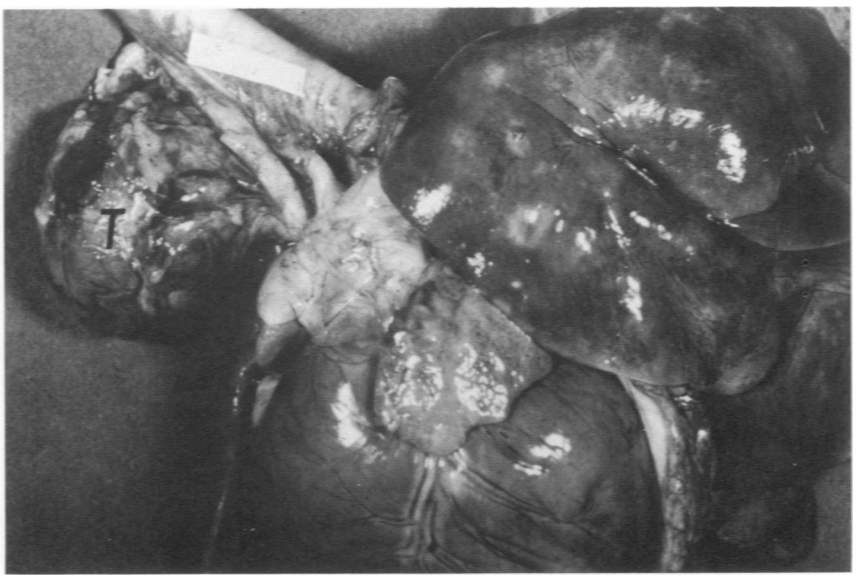

Figure 38—Metastasis of a papillary carcinoma of the lung to the thyroid. Note the presence of neoplastic emboli within interfollicular lymphatics and veins. There is accompanying fibrosis and atrophy of the gland. (H&E, × 150) **Figure 39**—Ectopic thyroid tumor (*T*) located cranial to the heart.

40

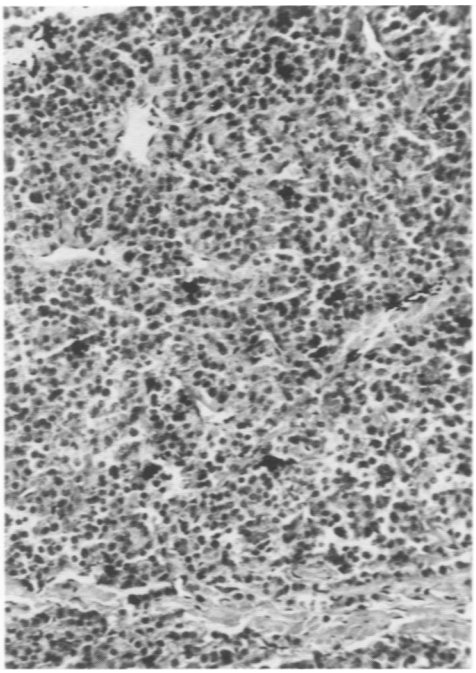

41

42

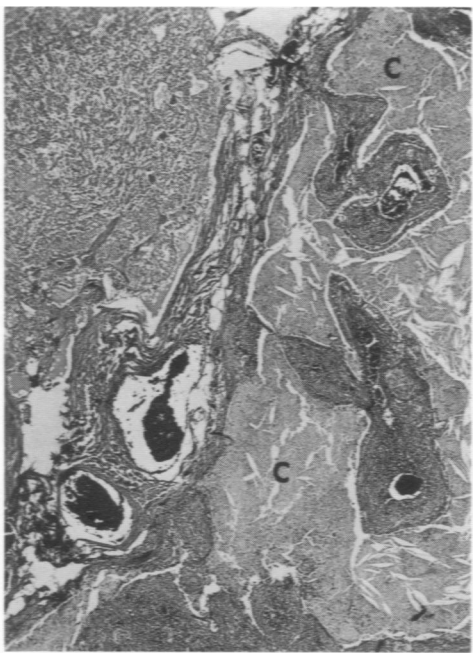

43

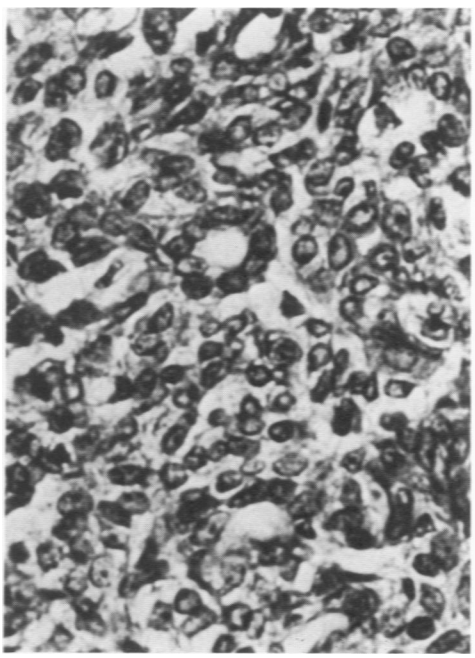

Figure 40—Ectopic thyroid tumor. A compact cellular pattern was present in most portions of this neoplasm. (H&E, × 150) **Figure 41**—Ectopic thyroid tumor. In other regions of the tumor, poorly formed follicles were evident. The neoplasm was intimately attached to the aorta. (H&E, × 140) **Figure 42**—Ectopic thyroid tumor associated with cysts. The cysts were filled with PAS-positive material and cholesterol clefts (*C*). The cyst lining was ciliated pseudostratified columnar epithelium. The solid portion of the tumor is seen along the upper left margin of this photomicrograph. (H&E, × 27) **Figure 43**—Cystic ectopic thyroid tumor. For the most part the neoplastic cells are arranged in sheets but occasionally form structures resembling microfollicles. (H&E, × 500)

44

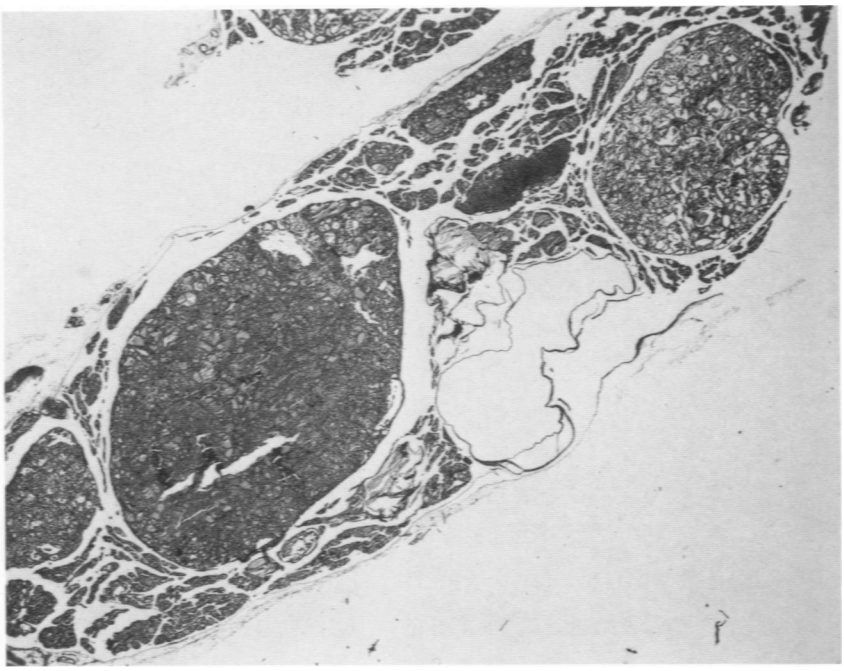

45

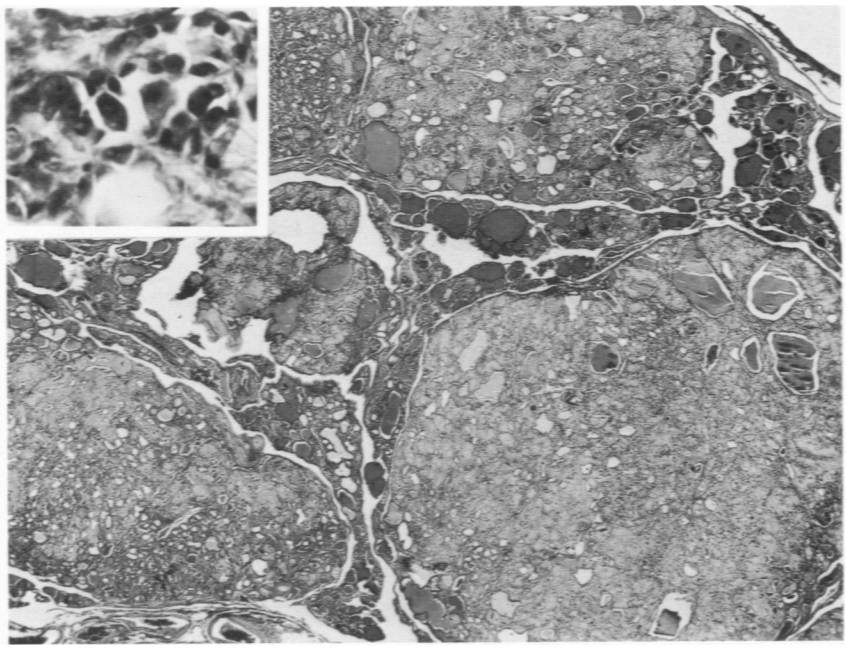

Figure 44—Multinodular adenomatous goiter of the feline thyroid. Nodules of irregularly arranged follicles are interspersed between normal thyroid parenchyma. (H&E, × 12) **Figure 45**—Amyloid-bearing multinodular adenomatous goiter of the feline thyroid. Note the presence of the hyalinized appearing amyloid within adenomatous nodules. (H&E, × 26) **Inset**—Pleomorphic cells were found within and between follicles (H&E, × 420).

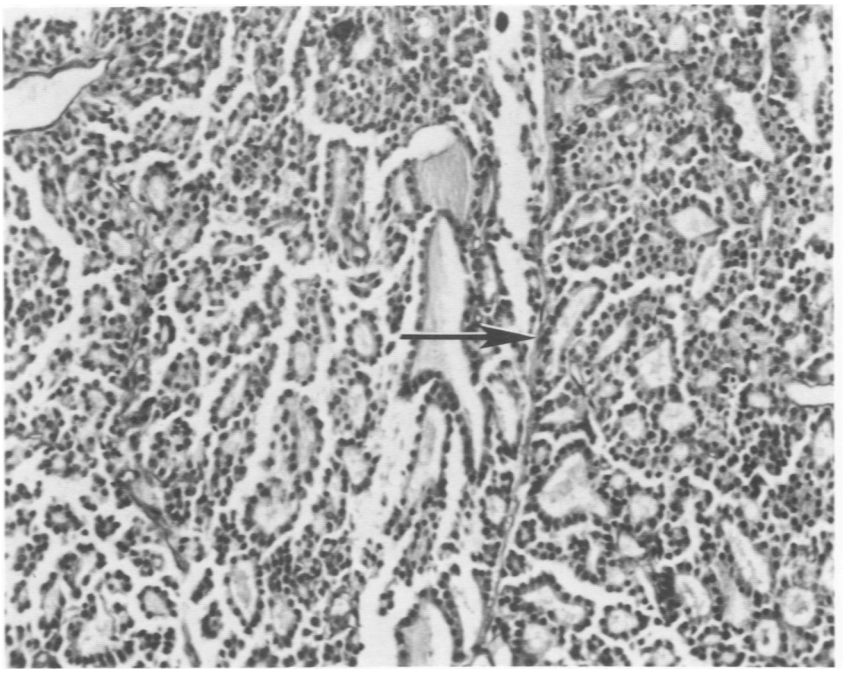

46

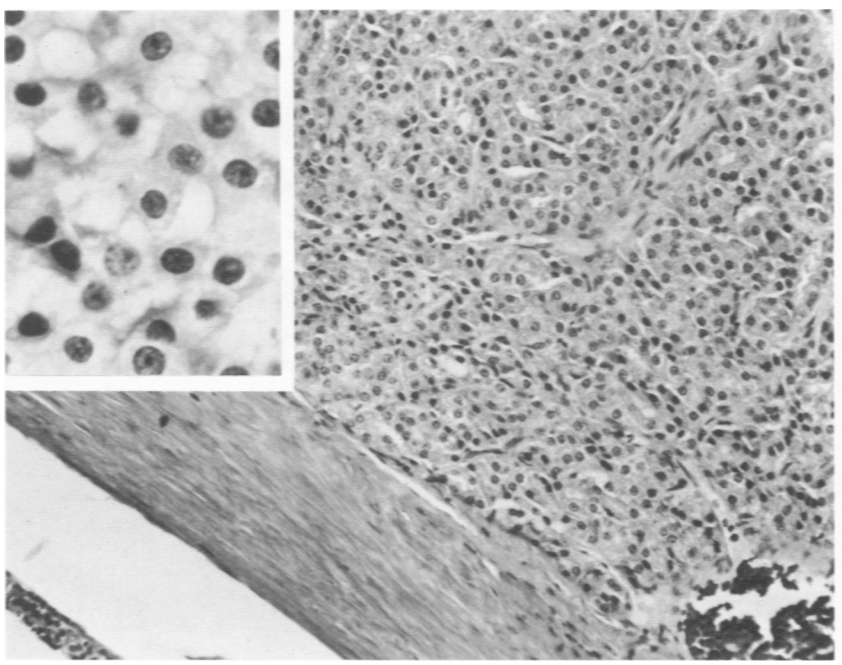

47

Figure 46—Typical adenoma of the feline thyroid. The tumor consists of irregularly arranged follicles. Deeper sections of this tumor revealed a lobular pattern formed by merging of partially encapsulated foci (*arrow*). (H&E, × 190) **Figure 47**—Atypical adenoma of the feline thyroid. Towards the capsular surface the follicular pattern is lost and the tumor appears compactly arranged. (H&E, × 190) **Inset**—A few atypical adenomas contained cells with large cytoplasmic vacuoles. (H&E, × 720)

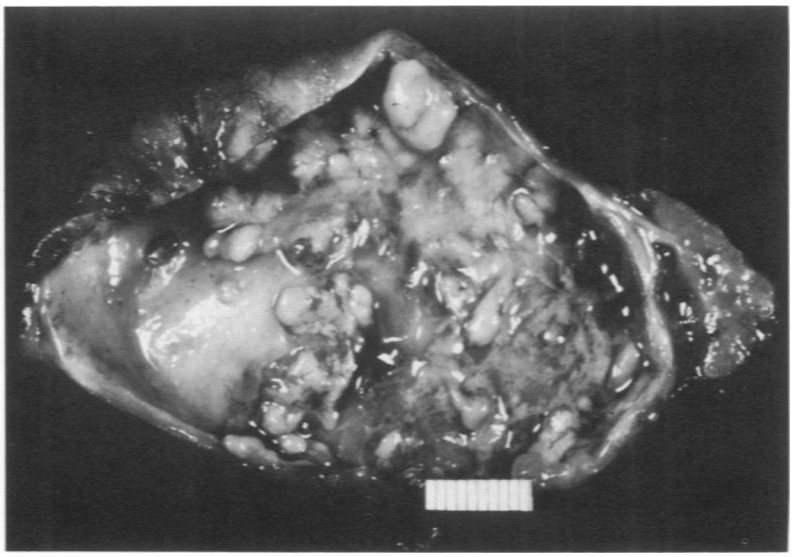

48

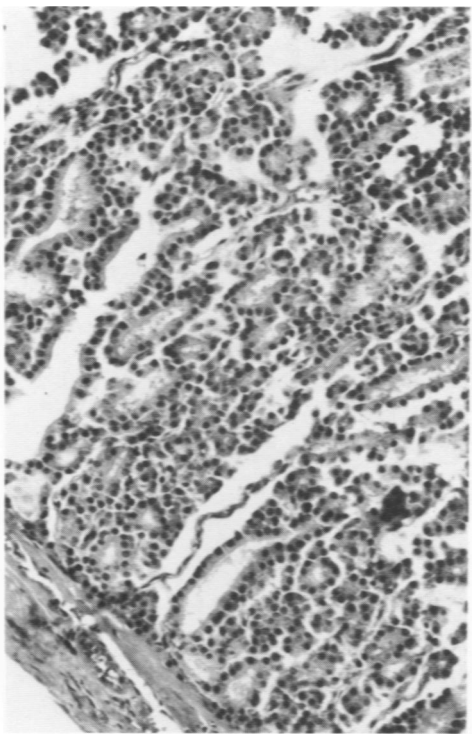

49

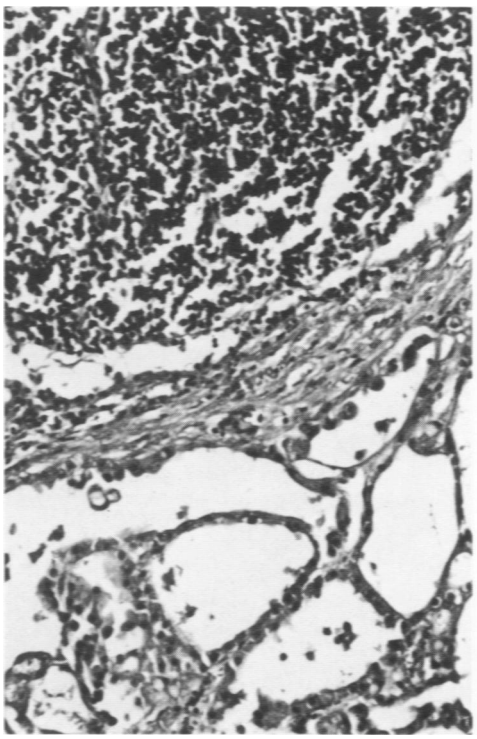

50

Figure 48—The cut surface of a cystic follicular carcinoma of the feline thyroid. Note the multinodular lining of the collapsed cyst. **Figure 49**—Well-differentiated follicular carcinoma of the feline thyroid. This malignant neoplasm is composed of irregularly arranged follicles. For the most part, the cells were uniform and closely resembled those of adenomas. (H&E, × 190) **Figure 50**—Metastasis of the tumor illustrated in Figure 49 to the retropharyngeal lymph node. The metastatic cells form distinct follicles. (H&E, × 190)

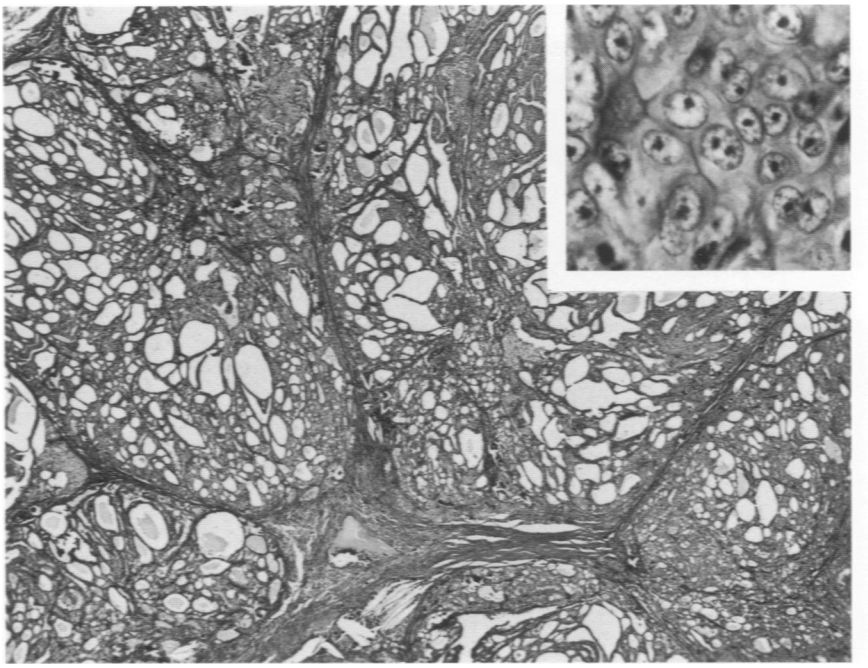

51

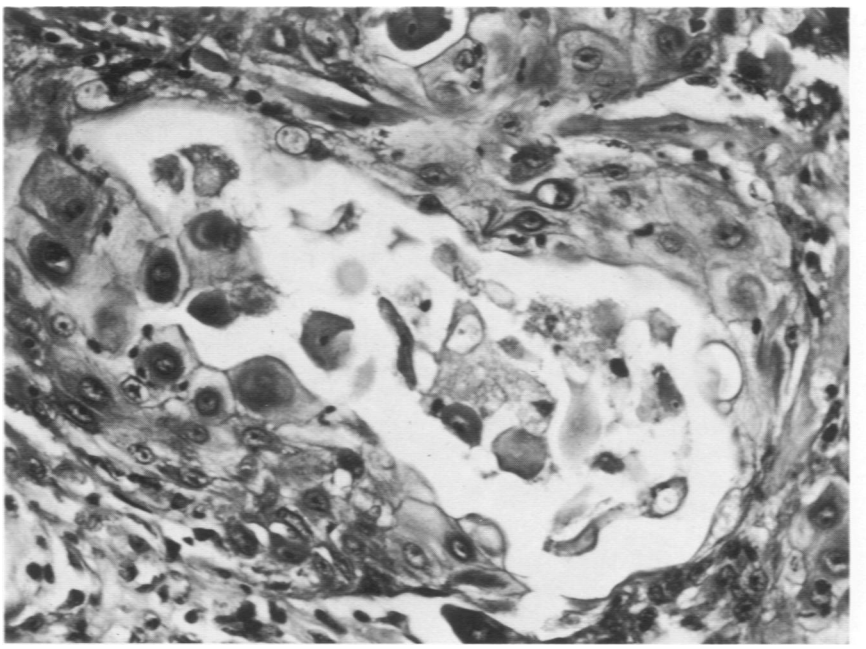

52

Figure 51—Follicular carcinoma of the feline thyroid. Note the division of this tumor by bands of fibrous connective tissue. A follicular pattern was found in most of the tumor. (H&E, × 26) **Inset**—In some regions the cells were compactly arranged. (H&E, × 560) **Figure 52**—Squamous metaplasia occurring within the follicular carcinoma illustrated in Figure 51. The cells have assumed a stratified squamous arrangement and some appear keratinized. (H&E, × 330)

53

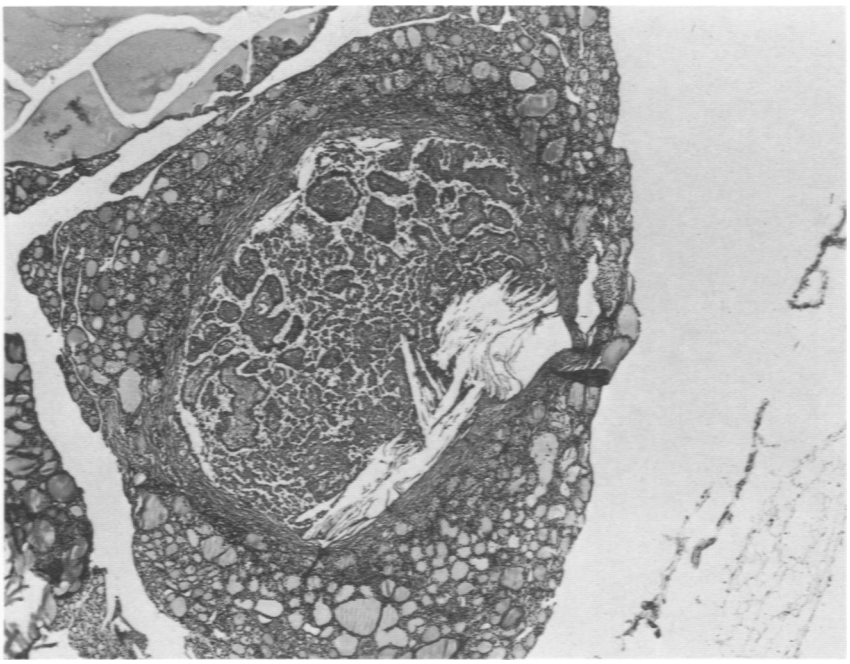

54

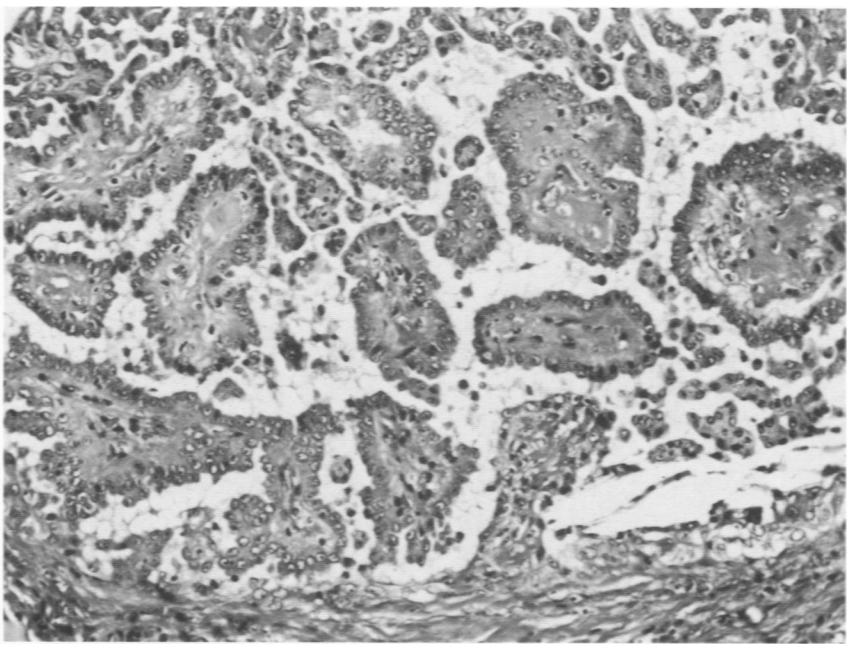

Figure 53—Papillary carcinoma of the feline thyroid. Note the papillary appearance of the tumor and the compression of adjacent tissue. (H&E, × 42) **Figure 54**—Papillary carcinoma of the feline thyroid. Fibrovascular fronds bear neoplastic cells with vesicular nuclei containing prominent nucleoli. (H&E, × 180)